**Blekinge Institute of Technology**
**Research Report No 2004:03**


# Design of Nonuniform Filter Banks with Frequency Domain Criteria

Jan Mark de Haan
Sven Nordholm
Ingvar Claesson

School of Engineering
Blekinge Institute of Technology

# Design of Nonuniform Filter Banks with Frequency Domain Criteria

J. M. de Haan[1], S. Nordholm[2], I. Claesson[1]

[1]Department of Telecommunications and Signal Processing
Blekinge Institute of Technology
Ronneby, Sweden

[2]Western Australia Telecommunications Research Institute
Perth, Australia

**Abstract**

This paper presents methods for the design of nonuniform filter banks. The filter bank structure is obtained from an uniformly modulated filter bank by using an allpass transform which has a lossless frequency function and a nonlinear phase function. The proposed design methods include linear and quadratic frequency domain criteria and linear constraints. Considered applications are subband adaptive filtering and subband coding. Analysis filter banks and synthesis filter banks are designed in two subsequent stages, and design objectives include minimization of subband aliasing as well as reconstruction output residual aliasing components on an individual basis. This way to formulate design objectives is appropriate for filter banks used in subband adaptive filtering. Other design objectives are to optimize the overall filter bank response for low amplitude and phase distortion. Designs with phase compensation for linear phase overall response are included. Examples are included of filter banks with increasing bandwidth.

# Chapter 1

# Introduction

Filter banks with the aliasing cancellation property have been of great interest in numerous applications, and design methods taking aliasing into account have been considered in an early stage [1, 2]. An overview is presented in [3]. However, aliasing cancellation filter banks are less suitable for subband adaptive filtering, since this property is not maintained when the subband signals are modified by individual subband filtering. This may lead to audible distortion in audio processing, especially when the individual aliasing terms have large magnitude. By appropriate minimization of aliasing terms, filter banks can be used in audio applications with subband domain filtering [4]. Examples of such audio application are noise suppression with single channels, for example spectral subtraction [5], or multiple channels, for example microphone arrays with subband beamforming [4]. Echo cancelling is not such an application since the near-end speech is not affected by subband filters. In [5] constrained adaption is used in combination with overlap techniques to avoid distortion and maintaining linear convolution properties. Earlier experiments have shown that such techniques are sensitive to fast variations of the adaptive coefficients giving audible echo effects in the output. Design methods for uniform DFT filter banks for subband adaptive filtering have been presented in [6].

Nonuniform filter banks have been of interest in speech enhancement, since by appropriate design it is possible to get a model, corresponding to the human auditory system [7]. They are also successfully applied to, speech recognition and speech coding. Nonuniform filter banks have also been proposed for subband adaptive filtering, e.g. in spectral subtraction for speech enhancement, [8], and beamforming for subband microphone arrays [9]. The filter banks addressed in this paper are nonuniform filter banks with polyphase structure. They utilize a lossless frequency transformation similar to a bilinear transform to obtain the non-uniformity [10]. These frequency transformed filter banks have previously been presented [11, 12], and are known to approximate the Bark frequency scale, or critical band scale, very accurately [7]. However, these filter banks are also known to cause phase distortion, which is inappropriate for coding or communications applications. The phase distortion can be compensated for by phase compensation filters [13].

Least Squares optimization techniques for the design of filter banks have previously been presented [14, 15]. Especially, a two stage Least Squares design procedure, where the analysis filter banks are designed first and the synthesis filter banks subsequently, is described in [16].

This paper proposes novel methods for the design of filter banks in two stages. First

a nonuniform analysis bank is designed and then a matching synthesis filter bank is designed, given the analysis filter bank. Two types of criteria have been used and evaluated: quadratic criteria and linear criteria, with our without linear constraints. The advantage of using linear criteria and constraints is that each frequency component can be individually controlled. A common aim is to design the analysis and synthesis banks with pre-specified parameters, such as number of subbands, filter lengths, delays and decimation factors. In the first stage the analysis filter bank is designed in such way that aliasing terms in the subbands are minimized. In the second stage the synthesis filter bank is designed, based on the analysis filter bank, such that the overall response is optimized and the reconstruction aliasing terms are minimized.

Generally, filter bank design methods are reduced to the design of a single prototype for the analysis and synthesis filter banks in order to obtain nearly perfect reconstruction properties. In the two stage design methods the amplitude distortion, phase distortion (delay) and aliasing distortion can be minimized or controlled for the analysis and synthesis filter banks separately. When using the linear criteria, they can be controlled for each frequency component individually, given a certain constraint.

In Chapter 2, a detailed description of the analysis and synthesis filter bank structure is given, as well as the properties of the analysis-synthesis system as a whole. Chapter 3 presents the design methods using unconstrained quadratic optimization (least squares), Chapter 4 presents the method using linear optimization with linear constraints and Chapter 5 presents the design methods using quadratic optimization with linear constraints. Design examples are included in these chapters. In Chapter 6 a discussion is given of all design examples. Chapter 7 discusses computational complexity and Chapter 8 concludes the paper.

# Chapter 2

# Filter Bank Structures

## 2.1 Frequency Transformed Filters

In frequency transformed filters, the unit sample delays are replaced by delay elements that have a lossless frequency function and nonlinear phase, and are implemented by recursive allpass filters. For the application in nonuniform filter banks, the first order allpass functions $Q(z)$ is considered

$$Q(z) = \frac{-\mu + z^{-1}}{1 - \mu z^{-1}}. \tag{2.1}$$

Using a real-valued coefficient in the range $-1 < \mu < 1$, a frequency dependent resolution can be obtained. The Fourier transform $Q(e^{j\omega})$ can be written as

$$Q(e^{j\omega}) = e^{j\rho(\omega)}, \tag{2.2}$$

with phase function

$$\rho(\omega) = -2 \arctan\left(\frac{1+\mu}{1-\mu}\tan\frac{\omega}{2}\right). \tag{2.3}$$

The group delay of $Q(z)$ is

$$\tau_Q(\omega) = -\rho'(\omega) = \frac{\frac{1+\mu}{1-\mu}\left(1+\tan^2\frac{\omega}{2}\right)}{1+\left(\frac{1+\mu}{1-\mu}\right)^2\tan^2\frac{\omega}{2}}, \tag{2.4}$$

where $\rho'(\omega)$ is the first derivative of the phase function $\rho(\omega)$. For derivations of the phase and group delay functions, see Appendix 9.1 and 9.2. Replacing the unit delays in digital filters by $Q(z)$ results in a transformation of the frequency response function according to

$$\omega' = \rho^{-1}(-\omega) = 2\arctan\left(\frac{1-\mu}{1+\mu}\tan\frac{\omega}{2}\right), \tag{2.5}$$

where $\rho^{-1}(\omega)$ is the inverse function of $\rho(\omega)$. The magnitude response is transformed towards angular frequency $\omega = 0$ for $\mu > 0$ or transformed towards $\omega = \pi$ for $\mu < 0$. Uniform resolution is obtained with $\mu = 0$, i.e. the allpass function reduces to the unit delay, $Q(z) = z^{-1}$. The frequency transformation function and the effect on a lowpass filter is illustrated in Fig. 2.1.

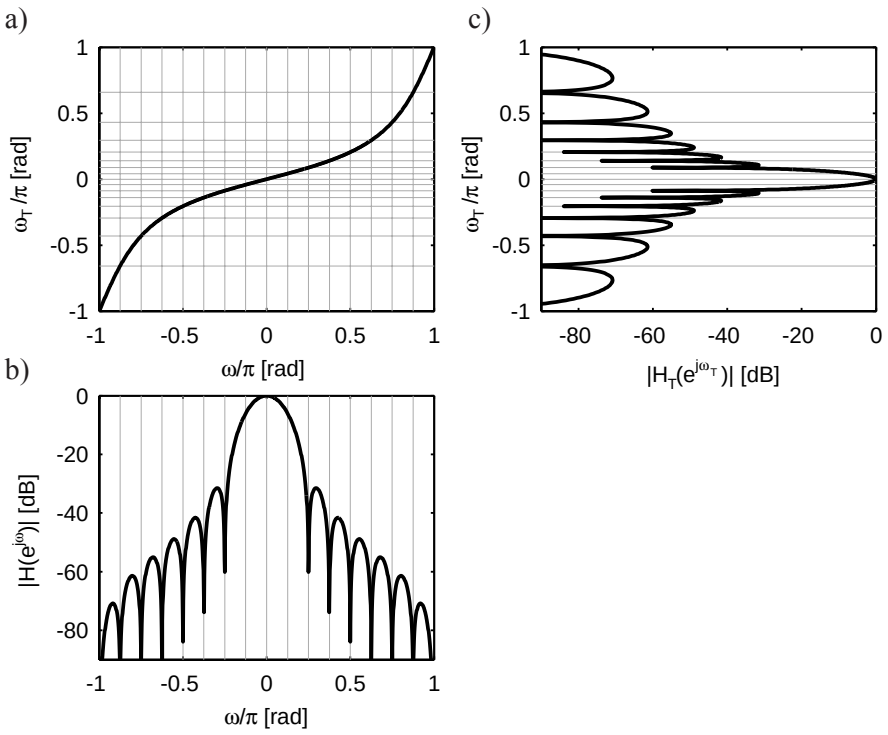


Figure 2.1: *Warping function* $\omega_T = \rho^{-1}(-\omega)$ *for* $\mu = 0.5$ *and the magnitude responses of a lowpass filter* $|H(e^{j\omega})|$ *and the transformed filter* $|H_T(e^{j\omega_T})|$*. The transformed filter is obtained by replacing the unit delays by* $Q(z)$*.*

## 2.2 Analysis Filter Bank Structure

A polyphase analysis filter bank structure with frequency transformation is considered. The analysis filter bank structure is based on the polyphase implementation of $M$-channel DFT filter banks, with a chain of allpass functions, polyphase filters and an IFFT operation, see Fig. 2.2. The analysis filters of a uniform $M$-channel DFT filter bank can be decomposed into polyphase components according to [3]

$$H_{m,\text{Uniform}}(z) = \sum_{l=0}^{M-1} A_l(z^M) z^{-l} W_M^{-ml}, \tag{2.6}$$

where $W_M = e^{-j2\pi/M}$ and $A_l(z)$ denote the polyphase components. The polyphase components are defined as

$$A_l(z) = \sum_{n=0}^{N-1} a_l(n) z^{-n}, \quad l = 0, \ldots, M-1, \tag{2.7}$$

where $a_l(n)$ are real polyphase component coefficients, $N$ is the number of polyphase component coefficients, $l$ is the polyphase component index and $M$ is the number of

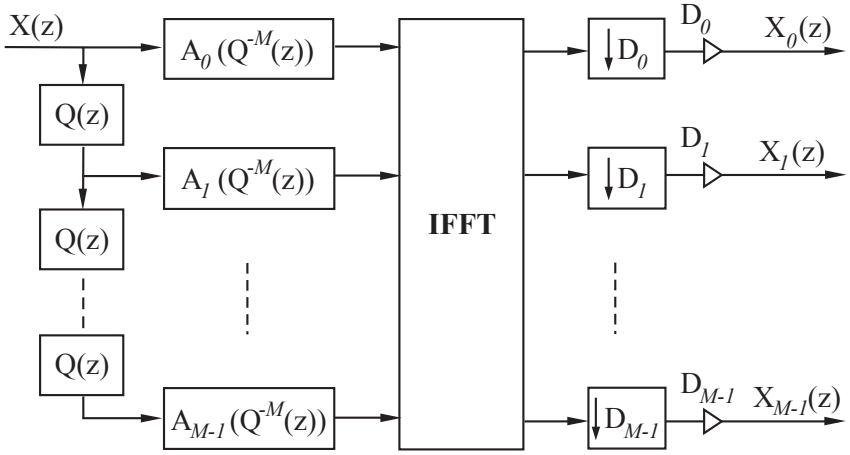


Figure 2.2: *Polyphase analysis filter bank structure with input signal $X(z)$ and subband signals $X_m(z), m = 0, \ldots, M-1$. The structure consists of a chain of allpass functions $Q(z)$, polyphase components $A_l(z), l = 0, \ldots, M-1$, an IFFT operation, and decimators with decimation rates $D_m$ and gain compensation.*

polyphase components, which is equal to the number of subbands.

Replacing the unit delays in Eq. (2.6) with first order allpass filters, i.e. $z^{-1} \rightarrow Q(z)$, yields analysis filters

$$H_m(z) = \sum_{l=0}^{M-1} A_l\left(Q^{-M}(z)\right) Q^l(z) W_M^{-ml}, \quad m = 0, \ldots, M-1. \tag{2.8}$$

Finally, $D_m$-fold decimators are applied to the corresponding subband signals, with a gain compensation corresponding to the decimation rate. The subband signals $X_m(z)$ are given by

$$X_m(z) = \sum_{d=0}^{D_m-1} H_m(z^{1/D_m} W_{D_m}^d) X(z^{1/D_m} W_{D_m}^d), \tag{2.9}$$

where $d$ is the aliasing term index.

The analysis filters in Eq. (2.8) can be described using the vector notation

$$H_m(z) = \boldsymbol{\phi}_m^T(z)\mathbf{a}, \tag{2.10}$$

where $(\cdot)^T$ denotes transpose. The composite polyphase component coefficient vector $\mathbf{a}$ is defined as

$$\mathbf{a} = \left[\mathbf{a}_0^T, \ldots, \mathbf{a}_{M-1}^T\right]^T, \tag{2.11}$$

with the polyphase component coefficient vectors

$$\mathbf{a}_l = [a_l(0), \ldots, a_l(N-1)]^T . \tag{2.12}$$

The basis function vector $\boldsymbol{\phi}_m(z)$ is defined as

$$\boldsymbol{\phi}_m(z) = \left[\boldsymbol{\phi}^T_{m,0}(z), \ldots, \boldsymbol{\phi}^T_{m,M-1}(z)\right]^T , \tag{2.13}$$

where

$$\boldsymbol{\phi}_{m,l}(z) = Q^l(z) W_M^{-ml} \left[1, Q^M(z), \ldots, Q^{(N-1)M}(z)\right]^T . \tag{2.14}$$

The vector notation provides a very compact writing and will be used for the problem formulation of the analysis filter bank design in Chapters 3.1, 4.1 and 5.1.

## 2.3 Compensation of Nonlinear Phase

The use of the allpass function in the analysis bank provides the frequency transformation but also introduces nonlinear phase, which is an undesired property in some applications. A phase compensation technique has been proposed in [13, 17]. This technique is considered in the filter banks addressed in this paper. Both filter banks with and without phase compensation are considered. Let $P(z)$ denote the allpass function for the synthesis filter bank. The synthesis filter bank without phase compensation has the same allpass functions as the analysis filter bank, i.e. $P(z) = Q(z)$. The most simplistic analysis-synthesis system with two channels using these allpass functions is illustrated in Fig. 2.3 a). The overall transfer function of the system given

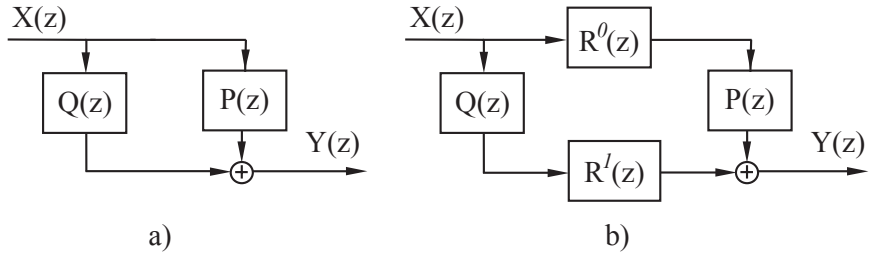


Figure 2.3: *(a) Two channel analysis-synthesis system without phase compensation, with* $P(z) = Q(z)$. *(b) Two channel analysis-synthesis system with phase compensation,* $P(z) \neq Q(z)$.

in Fig. 2.3 a) is $T(e^{j\omega}) = Q(e^{j\omega}) + P(e^{j\omega}) = 2e^{j\rho(\omega)}$ and has non-linear phase when $\mu \neq 0$. This two-channel system can be extended to $M$ channels, which results in the transfer function $T(e^{j\omega}) = Me^{j(M-1)\rho(\omega)}$.

In order to obtain a linear-phase transfer function, phase compensation filters can be

used. A two-channel system with phase compensation filters is given in Fig. 2.3 b). Let $P(z)$ be a unit delay, $P(e^{j\omega}) = e^{-j\omega}$, and $R^0(e^{j\omega}) = 1$, the ideal phase compensation filter for the second channel is given by $R^1_{\text{ideal}}(e^{j\omega}) = e^{-j\omega}Q^{-1}(e^{j\omega})$. Hence, the overall response is $T(e^{j\omega}) = Q(e^{j\omega})R_{\text{ideal}}(e^{j\omega}) + P(e^{j\omega}) = 2e^{-j\omega}$.

Since $Q^{-1}(e^{j\omega}) = Q(e^{-j\omega})$, the phase compensation filter $R_{\text{ideal}}(e^{j\omega})$ is either an unstable causal IIR filter or a stable non-causal IIR filter. The stable non-causal IIR filter can however be approximated by a causal FIR filter. More generally, let $P(z)$ be a $p$-sample delay, then the ideal phase compensation function is $R_{\text{ideal}}(e^{j\omega}) = e^{-j\omega p}Q(e^{-j\omega})$. Let the impulse response of $Q(e^{j\omega})$ be denoted by $q(n)$, then the impulse response of $R_{\text{ideal}}(e^{j\omega})$ is given by $r_{\text{ideal}}(n) = q(-n + p)$ and can be approximated for $n \geq 0$ by the FIR filter

$$R(z) = \sum_{n=0}^{p} r_{\text{ideal}}(n)z^{-n} = (1 - \mu z^{-1}) \sum_{n=0}^{p-1} \mu^{(p-n-1)} z^{-n}. \tag{2.15}$$

The product $Q(z)R(z) = z^{-p} - \mu^p$ approximates a $p$-sample delay, with closer approximation as $\mu^p$ approaches zero, thus for increasing $p$. The analysis-synthesis system with phase compensation in Fig. 2.3 b) can be extended to $M$ channels and the transfer function is approximately $T(e^{j\omega}) \approx Me^{-j(M-1)\omega p}$.

Since $Q(z)R(z) = z^{-p} - \mu^p$, a simple improvement is proposed by using $P(z) = z^{-p} + \mu^p$, which reduces the error and yields better approximation of a perfect reconstruction system. Observe that for a two channel system, the error is reduced to zero. The implications of this improvement in terms of the performance is studied in Chapters 3.4, 4.4 and 5.4.

## 2.4 Synthesis Filter Bank Structure

The polyphase synthesis filter bank structure consists of $D_m$-fold expanders, an FFT operation, polyphase components and a delay-and-sum chain of allpass functions, see Fig. 2.4. The synthesis filter bank has input subband signals $Y_0(z), \ldots, Y_{M-1}(z)$. The output signal is denoted by $Y(z)$, and is described in terms of the subband signals according to

$$Y(z) = \sum_{m=0}^{M-1} Y_m(z^{D_m})G_m(z). \tag{2.16}$$

In a uniform DFT synthesis filter bank, the synthesis filters can be decomposed into polyphase components according to [3]

$$G_{m,\text{Uniform}}(z) = \sum_{k=0}^{M-1} B_k(z^M)z^{-(M-1-k)}W_M^{-mk}, \tag{2.17}$$

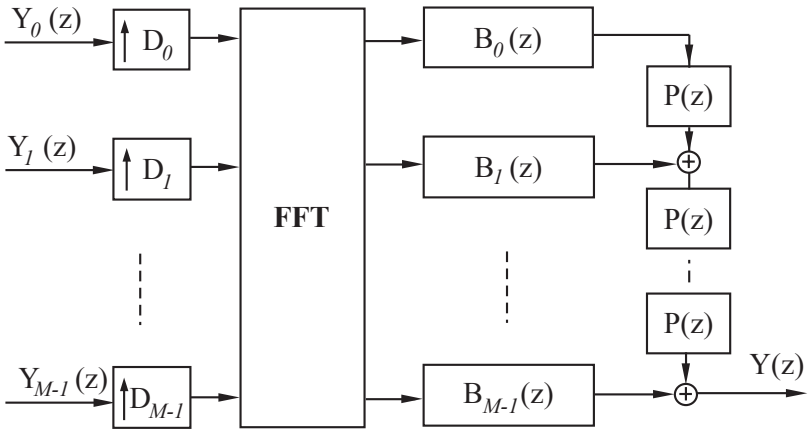


Figure 2.4: *Polyphase synthesis filter bank structure with input subband signals* $Y_m(z), m = 0, \ldots, M-1$ *and output signal* $Y(z)$*. The structure consists of interpolators, an FFT operation, polyphase components* $B_l(z)$*,* $l = 0, \ldots, M-1$*, and a delay-and-sum line with filters* $P(z)$*.*

In the nonuniform case, the unit delays in the delay-and-sum chain are replaced by $P(z)$ and the polyphase components are denoted $B_k(z)$ instead of $B_k(z^M)$, for simplicity. Thus, the polyphase decomposition of the synthesis filters is given by

$$G_m(z) = \sum_{k=0}^{M-1} B_k(z) P^{(M-1-k)}(z) W_M^{-mk}. \tag{2.18}$$

The polyphase components $B_k(z)$ are defined as

$$B_k(z) = \sum_{n=0}^{L-1} b_k(n) P^{Mn}(z) R^{M(L-n-1)+k}(z), \qquad k = 0, \ldots, M-1, \tag{2.19}$$

where $b_k(n)$ are real polyphase component coefficients. With this definition, both linear phase and non-linear phase overall transfer functions can be obtained, depending on how $P(z)$ and $R(z)$ are chosen.

The synthesis filters in Eq. (2.18) can be described by the vector notation

$$G_m(z) = \boldsymbol{\varphi}_m^T(z)\mathbf{b}, \tag{2.20}$$

where $(\cdot)^T$ denotes transpose. The composite polyphase component coefficient vector is defined as

$$\mathbf{b} = \left[\mathbf{b}_0^T, \ldots, \mathbf{b}_{M-1}^T\right]^T, \tag{2.21}$$

with the polyphase component coefficient vectors

$$\mathbf{b}_k = \left[b_k(0), \ldots, b_k(L-1)\right]^T. \tag{2.22}$$

The basis function vector $\boldsymbol{\varphi}_m(z)$ is defined as

$$\boldsymbol{\varphi}_m(z) = \left[\boldsymbol{\varphi}_{m,0}^T(z), \ldots, \boldsymbol{\varphi}_{m,M-1}^T(z)\right]^T, \tag{2.23}$$

where

$$\boldsymbol{\varphi}_{m,k}(z) = P(z)^{(M-1-k)} R^k(z) W_M^{mk} \begin{pmatrix} R^{(L-1)}(z) \\ P^M(z) R^{(L-2)}(z) \\ \ldots \\ P^{(L-2)M}(z) R(z) \\ P^{(L-1)M}(z) \end{pmatrix}. \tag{2.24}$$

The vector notation will be used for the problem formulation of the synthesis filter bank design in Chapters 3.2, 4.2, and 5.2.

## 2.5 Overall Transfer Functions

The design of the synthesis filters intends to aim at the properties of the analysis and synthesis filter banks as a whole. These properties are derived in this section. The filter bank output $Y(z)$ expressed in terms of the input $X(z)$, with the analysis and synthesis filter banks connected $Y_m(z) = X_m(z)$, is given by

$$Y(z) = \sum_{m=0}^{M-1} G_m(z) \sum_{d=0}^{D_m-1} X(zW_{D_m}^d) H_m(zW_{D_m}^d). \tag{2.25}$$

This can be rewritten as

$$Y(z) = T(z)X(z) + \sum_{m=0}^{M-1} \sum_{d=1}^{D_m-1} S_{m,d}(z) X(zW_{D_m}^d), \tag{2.26}$$

where the overall transfer function $T(z)$ affects the linear term in the output signal and the aliasing transfer functions $S_{m,d}(z)$ affect the undesired aliasing terms, which are modulated versions of the input signal. The overall transfer function is given by

$$T(z) = \sum_{m=0}^{M-1} H_m(z) G_m(z). \tag{2.27}$$

Using the vector notations for $H_m(z)$ and $G_m(z)$ in Eqs. (2.10), and (2.20), respectively, the overall transfer function in Eq. (2.27) can be written as

$$T(z) = \mathbf{a}^T \left\{ \sum_{m=0}^{M-1} \boldsymbol{\phi}_m(z) \boldsymbol{\varphi}_m^T(z) \right\} \mathbf{b}, \tag{2.28}$$

which can be reduced to

$$T(z) = \boldsymbol{\psi}^T(z) \mathbf{b}, \tag{2.29}$$

where

$$\boldsymbol{\psi}(z) = \left\{ \sum_{m=0}^{M-1} \boldsymbol{\varphi}_m(z) \boldsymbol{\phi}_m^T(z) \right\} \mathbf{a}. \tag{2.30}$$

The aliasing transfer functions $S_{m,d}(z)$ are defined by

$$S_{m,d}(z) = H_m(zW_{D_m}^d) G_m(z) = \boldsymbol{\xi}_{m,d}^T(z) \mathbf{b}, \tag{2.31}$$

where

$$\boldsymbol{\xi}_{m,d}(z) = \boldsymbol{\varphi}_m(z) \boldsymbol{\phi}_m^T(zW_{D_m}^d) \mathbf{a}. \tag{2.32}$$

Note that the overall transfer function $T(z)$ can be written in terms of the aliasing transfer functions $S_{m,d}(z)$ according to

$$T(z) = \sum_{m=0}^{M-1} S_{m,d=0}(z). \tag{2.33}$$

# Chapter 3

# Unconstrained Quadratic Optimization

## 3.1 Analysis Filter Bank Design

The quadratic (least squares) frequency domain design criterion for the analysis filter bank is described in this section. For all analysis filters, a passband region $\Omega_m^{\mathcal{P}}$ and a stopband region $\Omega_m^{\mathcal{S}}$ are defined. In the uniform case, the center frequencies of the analysis filters are $\omega_m^{\mathcal{C}} = 2\pi m/M$. In the nonuniform case, the center frequencies are transformed according to Eq. (2.5), $\omega_m^{\mathcal{C}} = \rho^{-1}(-2\pi m/M)$. The passband region is defined in the vicinity of the center frequencies as

$$\Omega_m^{\mathcal{P}} = \left[\rho^{-1}\left(-\tfrac{2\pi m-\delta\pi}{M}\right), \rho^{-1}\left(-\tfrac{2\pi m+\delta\pi}{M}\right)\right], \tag{3.1}$$

where the factor $0 < \delta \leq 1$ controls the width of the passband region. Since the main-lobe in the uniform case is approximately $1/M$–th of the frequency range, the passbands are discretized into $I/M + 1$ frequency points according to

$$\Omega_m^{\mathcal{P}} = \rho^{-1}\left(-2\pi\left(m + \delta\left(\tfrac{i}{I/M+1} - \tfrac{1}{2}\right)/M\right)\right) \qquad i = 0, \ldots, \tfrac{I}{M} + 1 \tag{3.2}$$

where the use of the frequency transformation function ensures a spacing which is nonuniform and dependent on $\mu$. The total number of frequency points for all passbands is $M(I/M + 1) = I + M$.

The stopbands $\Omega_m^{\mathcal{S}}$ depend on the decimation rates $D_m$ and for each analysis filter, the stopband boundaries are set $\pi/D_m$ around the center of the main lobe. Due to the frequency transformation with $\mu \neq 0$, these center frequencies will not be the same as the transformed uniform center frequencies. In the uniform ideal filter case, the stopband boundaries are $\pi/M$ around the center frequency. The center frequencies in the nonuniform case can be found by taking the mean of the transformed ideal boundaries of the uniform case

$$\overline{\omega}_m^{\mathcal{C}} = \tfrac{1}{2}\rho^{-1}\left(-\tfrac{2\pi m-\pi}{M}\right) + \tfrac{1}{2}\rho^{-1}\left(-\tfrac{2\pi m+\pi}{M}\right) \tag{3.3}$$

The stopbands are then defined using these center frequencies according to

$$\Omega_m^{\mathcal{S}} = \left[\overline{\omega}_m^{\mathcal{C}} - \pi, \overline{\omega}_m^{\mathcal{C}} - \tfrac{\pi}{D_m}\right] \cup \left[\overline{\omega}_m^{\mathcal{C}} + \tfrac{\pi}{D_m}, \overline{\omega}_m^{\mathcal{C}} + \pi\right], . \tag{3.4}$$

Since the stopbands comprise a larger part of the frequency range relative to the passbands, the stopbands are discretized into a set of $I(M-1)/M$ frequency points with

nonuniform spacing. This can be done by transforming the boundaries back to the uniform domain, create a set of uniformly spaced points between these boundaries and transform to get a nonuniform spacing. The total number of frequency points in all stopbands is $MI(M-1)/M$, which is $I(M-1)$.

The desired analysis filter frequency response $H_m^{\mathcal{D}}(e^{j\omega})$ is defined as

$$H_m^{\mathcal{D}}(e^{j\omega}) = \begin{cases} e^{j\rho(\omega)\Delta_A} & \text{for } \omega \in \Omega_m^{\mathcal{P}} \\ 0 & \text{for } \omega \in \Omega_m^{\mathcal{S}} \\ \text{undefined} & \text{otherwise} \end{cases} \tag{3.5}$$

with desired magnitude and delay. The delay

$$\tau_{H_m} = -\rho'(\omega)\Delta_A, \tag{3.6}$$

where $'$ denotes the first derivative, is controlled by the constant $\Delta_A$. With $\mu = 0$ (the uniform case), and $\Delta_A = (MN-1)/2$, linear phase analysis filters will be obtained.

The analysis filter bank design problem is formulated as follows,

$$\mathbf{a}_{\text{opt}} = \arg\min_{\mathbf{a}} \left\{ J_A(\mathbf{a}) = J_A^{I}(\mathbf{a}) + J_A^{II}(\mathbf{a}) \right\}, \tag{3.7}$$

i.e. the analysis polyphase filter coefficients $\mathbf{a}_{\text{opt}}$ minimize a sum of two quadratic forms. The first term is the passband cost function

$$J_A^{I}(\mathbf{a}) = \frac{1}{I+M} \sum_{m=0}^{M-1} \sum_{\omega \in \Omega_m^{\mathcal{P}}} \left| H_m(e^{j\omega}) - H_m^{\mathcal{D}}(e^{j\omega}) \right|^2, \tag{3.8}$$

which is normalized with the total number of frequency points for the passbands. The second term is the stopband cost function

$$J_A^{II}(\mathbf{a}) = \frac{1}{I(M-1)} \sum_{m=0}^{M-1} \sum_{\omega \in \Omega_m^{\mathcal{S}}} \left| H_m(e^{j\omega}) \right|^2, \tag{3.9}$$

which is normalized with the total number of frequency points for the stopbands. Minimizing the sum of the cost functions yields analysis filters with optimal passband characteristics and low aliasing levels due to the stopband attenuation.

The vector notation for $H_m(e^{j\omega})$ in Eq. (2.10) can be used, with basis function matrices for the passband regions

$$\mathbf{\Phi}_m^{\mathcal{P}} = \tfrac{1}{\sqrt{I+M}} \left[ \boldsymbol{\phi}_m(e^{j\omega_{m,0}^{\mathcal{P}}}), \ldots, \boldsymbol{\phi}_m(e^{j\omega_{m,I/M}^{\mathcal{P}}}) \right]^T, \tag{3.10}$$

and corresponding desired response vectors

$$\mathbf{H}_m^{\mathcal{D}} = \frac{1}{\sqrt{I+M}} \left[ H_m^{\mathcal{D}}(e^{j\omega_{m,0}^{\mathcal{P}}}), \ldots, H_m^{\mathcal{D}}(e^{j\omega_{m,I/M}^{\mathcal{P}}}) \right]^T. \tag{3.11}$$

Eq. (3.8) can be rewritten as

$$J_A^I(\mathbf{a}) = \sum_{m=0}^{M-1} \parallel \mathbf{\Phi}_m^{\mathcal{P}} \mathbf{a} - \mathbf{H}_m^{\mathcal{D}} \parallel^2, \tag{3.12}$$

which leads to the quadratic form

$$J_A^I(\mathbf{a}) \;=\; \mathbf{a}^T \left\{ \sum_{m=0}^{M-1} \mathbf{\Phi}_m^{\mathcal{P}\,H} \mathbf{\Phi}_m^{\mathcal{P}} \right\} \mathbf{a} - 2\mathbf{a}^T \left\{ \sum_{m=0}^{M-1} \mathrm{Re}\{\mathbf{\Phi}_m^{\mathcal{P}\,H} \mathbf{H}_m^{\mathcal{D}}\} \right\} + 1, \tag{3.13}$$

where $(\cdot)^H$ denotes conjugate transpose and $\mathrm{Re}\{\cdot\}$ is the real operator. Introducing basis function matrices for the stopband regions

$$\mathbf{\Phi}_m^{\mathcal{S}} = \frac{1}{\sqrt{I(M-1)}} \left[ \boldsymbol{\phi}_m(e^{j\omega_{m,0}^{\mathcal{S}}}), \ldots, \boldsymbol{\phi}_m(e^{j\omega_{m,I(M-1)/M}^{\mathcal{S}}}) \right]^T, \tag{3.14}$$

Eq. (3.9) can be rewritten to

$$J_A^{II}(\mathbf{a}) = \sum_{m=0}^{M-1} \parallel \mathbf{\Phi}_m^{\mathcal{S}} \mathbf{a} \parallel^2, \tag{3.15}$$

which leads to the quadratic form

$$J_A^{II}(\mathbf{a}) = \mathbf{a}^T \left\{ \sum_{m=0}^{M-1} \mathbf{\Phi}_m^{\mathcal{S}\,H} \mathbf{\Phi}_m^{\mathcal{S}} \right\} \mathbf{a} \tag{3.16}$$

The real-valued solution $\mathbf{a}_{\text{opt}}$ in Eq. (3.7) is found by setting the gradient of the cost function equal to zero, i.e. by solving the normal equations

$$\sum_{m=0}^{M-1} \mathrm{Re} \left\{ \mathbf{\Phi}_m^{\mathcal{P}\,H} \mathbf{\Phi}_m^{\mathcal{P}} + \mathbf{\Phi}_m^{\mathcal{S}\,H} \mathbf{\Phi}_m^{\mathcal{S}} \right\} \mathbf{a}_{\text{opt}} = \sum_{m=0}^{M-1} \mathrm{Re} \left\{ \mathbf{\Phi}_m^{\mathcal{P}\,H} \mathbf{H}_m^{\mathcal{D}} \right\}. \tag{3.17}$$

## 3.2 Synthesis Filter Bank Design

The quadratic design criterion for the synthesis filter bank design is described in this section. When non-linear phase is allowed, the desired overall filter bank response $T^{\mathcal{D}}(e^{j\omega})$ is given by

$$T^{\mathcal{D}}(e^{j\omega}) = e^{j\rho(\omega)\Delta_S}, \tag{3.18}$$

and no phase compensation is used, i.e. $P(z) = Q(z)$ and $R(z) = 1$. The desired overall delay is $\tau_T(\omega) = -\rho'(\omega)\Delta_S$. In the case of linear phase, the desired overall response is given by

$$T^{\mathcal{D}}(e^{j\omega}) = e^{-j\omega p\Delta_S}, \tag{3.19}$$

with phase compensation, i.e. when the functions $P(z)$ and $R(z)$ are chosen as described in Chapter 2.3. In this case, the desired overall delay is $\tau_T(\omega) = p\Delta_S$. In both cases, the overall filter bank delay is controlled with the constant $\Delta_S$. With $\mu = 0$ and $p = 1$, which is the uniform case, $\Delta_S$ represents the overall filter bank delay. In the case of linear phase analysis and synthesis filters, the delay is $\Delta_S = M(N+L)/2-1$.

The synthesis filter bank design criterion is formulated as follows

$$\mathbf{b}_{\text{opt}} = \arg\min_{\mathbf{b}} \left\{ J_S(\mathbf{b}) = J_S^{I}(\mathbf{b}) + J_S^{II}(\mathbf{b}) \right\}. \tag{3.20}$$

The synthesis filter coefficients $\mathbf{b}_{\text{opt}}$ minimize a sum of two quadratic forms. The first term is the overall response cost function

$$J_S^{I}(\mathbf{b}) = \frac{1}{I} \sum_{\omega\in\Omega} \left| T(e^{j\omega}) - T^{\mathcal{D}}(e^{j\omega}) \right|^2, \tag{3.21}$$

which is normalized by the number of frequency points. The second term is the aliasing cost function

$$J_S^{II}(\mathbf{b}) = \frac{1}{IM} \sum_{m=0}^{M-1} \frac{1}{D_m - 1} \sum_{d=1}^{D_m-1} \sum_{\omega\in\Omega} \left| S_{m,d}(e^{j\omega}) \right|^2, \tag{3.22}$$

which is normalized by the number of frequency points, the number of subbands and the number of aliasing terms. The optimization frequency interval is $\Omega = [-\pi, \pi]$, which is discretized to frequency points $\omega_i$, $i = 0, \ldots, I-1$, using a nonuniform spacing according to the frequency transformation function. The optimization criterion yields an optimized overall transfer function $T(z)$ and independently minimized aliasing transfer functions $S_{m,d}(z), \forall m, \forall d > 0$.

The overall response cost function $J_S^{I}(\mathbf{b})$ in Eq. (3.21) can be rewritten using the vector notation of $T(z)$ in Eq. (2.29) and by introducing basis function matrix

$$\mathbf{\Psi} = \tfrac{1}{\sqrt{I}} \left[ \boldsymbol{\psi}(e^{j\omega_0}), \ldots, \boldsymbol{\psi}_m(e^{j\omega_{I-1}}) \right]^T, \tag{3.23}$$

and the desired response vector

$$\mathbf{T}^{\mathcal{D}} = \tfrac{1}{\sqrt{I}} \left[ T^{\mathcal{D}}(e^{j\omega_0}), \ldots, T^{\mathcal{D}}(e^{j\omega_{I-1}}) \right]^T, \tag{3.24}$$

according to

$$J_S^{I}(\mathbf{b}) = \| \mathbf{\Psi}\mathbf{b} - \mathbf{T}^{\mathcal{D}} \|^2, \tag{3.25}$$

which finally yields the quadratic form

$$J_S^I(\mathbf{b}) = \mathbf{b}^T \mathbf{\Psi}^H \mathbf{\Psi} \mathbf{b} - 2\mathbf{b}^T \mathrm{Re}\{\mathbf{\Psi}^H \mathbf{T}^{\mathcal{D}}\} + 1. \tag{3.26}$$

The aliasing cost function $J_S^{II}(\mathbf{b})$ in Eq. (3.22) can be compactly written using the vector notation of $S_{m,d}(z)$ in Eq. (2.31), and by introducing basis function matrix

$$\mathbf{\Xi}_{m,d} = \frac{1}{\sqrt{IM(D_m-1)}} \left[ \boldsymbol{\xi}_{m,d}(e^{j\omega_0}), \ldots, \boldsymbol{\xi}_{m,d}(e^{j\omega_{I-1}}) \right]^T, \tag{3.27}$$

according to

$$J_S^{II}(\mathbf{b}) = \sum_{m=0}^{M-1} \sum_{d=1}^{D_m-1} \parallel \mathbf{\Xi}_{m,d} \mathbf{b} \parallel^2, \tag{3.28}$$

which yields the quadratic form

$$J_S^{II}(\mathbf{b}) = \mathbf{b}^T \mathbf{\Lambda} \mathbf{b} \tag{3.29}$$

where

$$\mathbf{\Lambda} = \sum_{m=0}^{M-1} \sum_{d=1}^{D_m-1} \mathbf{\Xi}_{m,d}^H \mathbf{\Xi}_{m,d}. \tag{3.30}$$

The real-valued solution $\mathbf{b}_{\text{opt}}$ which minimizes $J_S(\mathbf{b})$ is found by solving the normal equations

$$\mathrm{Re}\left\{ \mathbf{\Psi}^H \mathbf{\Psi} + \mathbf{\Lambda} \right\} \mathbf{b}_{\text{opt}} = \mathrm{Re}\left\{ \mathbf{\Psi}^H \mathbf{T}^{\mathcal{D}} \right\}, \tag{3.31}$$

## 3.3 Design Examples

In this section, design examples of filter banks are presented with and without phase compensation. Analysis filter banks and matching synthesis filter banks with $M = 8$ subbands are designed. The bandwidth of the subbands increases proportional to frequency, and the decimation factors are set to $D_m = \{8, 6, 4, 2, 2, 2, 4, 6\}$. The allpass function coefficient is set so that the value of the cost function in the analysis filter bank design is low, $\mu = 0.4$, see Chapter 3.4. Using this value of the allpass coefficient, the bandwidth compression around $\omega = 0$ is approximately $230\%$ and the bandwidth expansion around $\omega = \pi$ is approximately $260\%$. The number of coefficients in the polyphase filters for the analysis and synthesis filter bank are $N = 4$, and $L = 4$, respectively. The passband parameter in the analysis filter bank design is set to $\delta = \frac{1}{4}$. The delay parameters are set to $\Delta_A = (MN-1)/2$ and $\Delta_S = M(N+L)/2 - 1$. The number of frequency points in the designs is $I = 10MN$ and $I = 10ML$, respectively. The cost function values for all design examples are summarized in Table 6.

### 3.3.1 Example without Phase Compensation - LS[1]

Filter banks were designed without phase compensation in the synthesis filter bank. The resulting analysis filters $H_m(z)$ and synthesis filters $G_m(z)$ are shown in Fig. 3.1. It can be seen that the stopbands of the analysis and synthesis filters exhibit typical minimum energy characteristics. The magnitude response and the group delay of the overall response, $T(e^{j\omega})$, and the average magnitude of all undesired aliasing terms

$$S_{\text{avg}}(\omega) = \frac{1}{M} \sum_{m=0}^{M-1} \frac{1}{D_m - 1} \sum_{m=1}^{D_m-1} \left| S_{m,d}(e^{j\omega}) \right|^2, \tag{3.32}$$

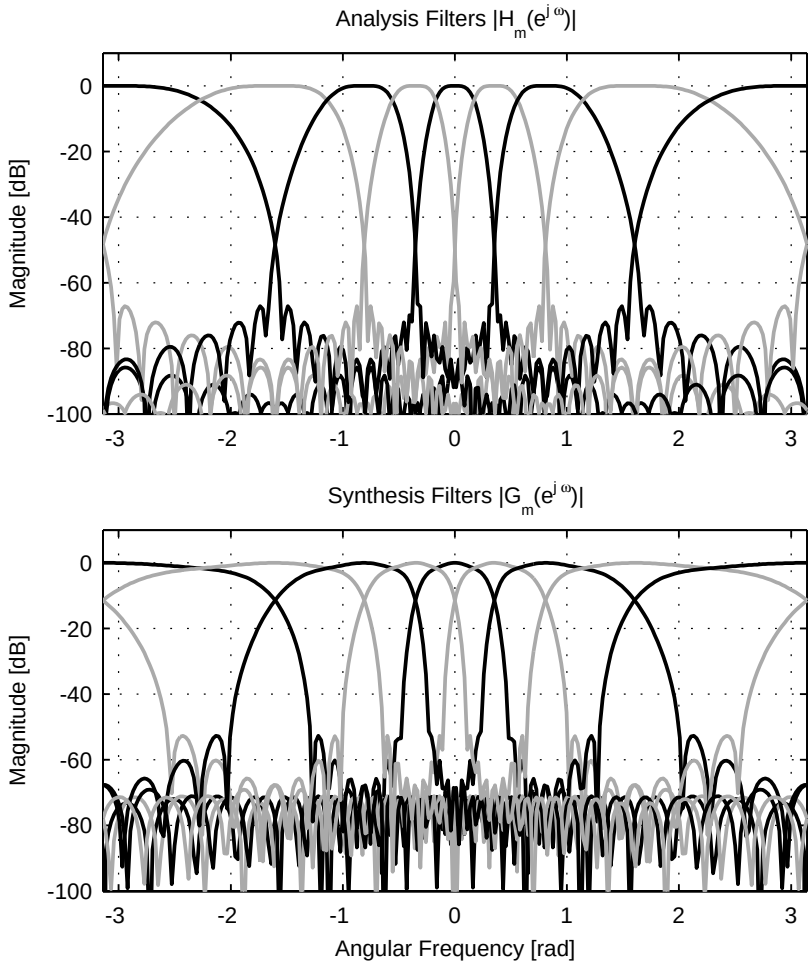


Figure 3.1: **Design Example LS**[1]. *Magnitude responses of the analysis filters* $|H_m(e^{j\omega})|$ *and synthesis filters* $|G_m(e^{j\omega})|$*, for* $m = 0, \ldots, M-1$*. The analysis and synthesis filter banks are designed with unconstrained quadratic optimization. There is no phase compensation in the synthesis filter bank. The cost function values for the analysis filter bank design are* $J_A^I(\mathbf{a}) = -78.4$ *dB and* $J_A^{II}(\mathbf{b}) = -70.9$ *dB.*

is shown in Fig. 3.2. The cost function values are summarized in Table 6. The ripple in the overall magnitude response is approximately $73 \cdot 10^{-3}$ dB and minimum aliasing attenuation is approximately $60$ dB. The delay $\tau_T(\omega)$ of the overall filter bank is between 13 and 72 samples.

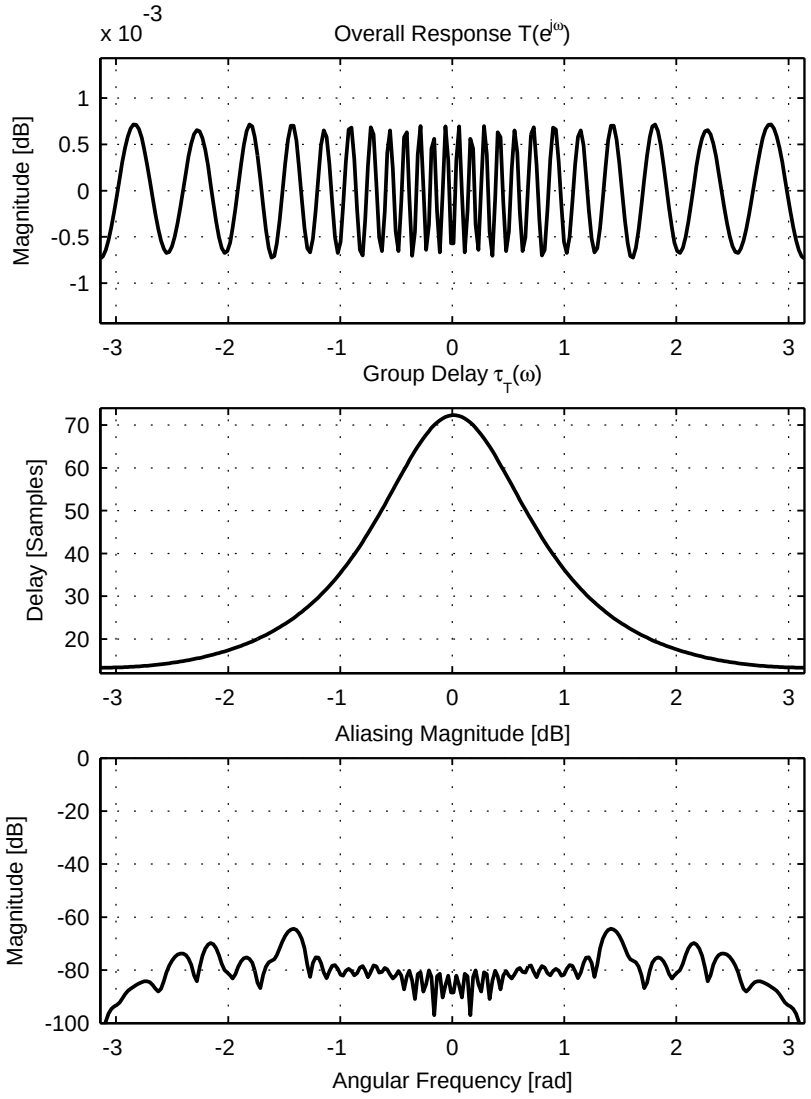


Figure 3.2: **Design Example LS**[1]. *Overall magnitude response $|T(e^{j\omega})|$, group delay and maximum output signal aliasing magnitude $S_{avg}(\omega)$. The cost function values for the synthesis filter bank design are $J_S^I(\mathbf{b}) = -84.9$ dB and $J_S^{II}(\mathbf{b}) = -76.2$ dB.*

### 3.3.2 Example with Phase Compensation - LS$^2$

Filter banks were designed with phase compensation in the synthesis filter bank. The delay parameter for the phase compensation was set to $p = 6$, and $P(z) = z^{-p} + \mu^p$. The resulting analysis filters $H_m(z)$ and synthesis filters $G_m(z)$ are shown in Fig. 3.3. The magnitude and the group delay of the overall response, $T(e^{j\omega})$ and the average magnitude of all aliasing terms $S_{\text{avg}}(\omega)$ are shown in Fig. 3.4. The cost function values are summarized in Table 6. The ripple in the overall magnitude response is approximately $1 \cdot 10^{-2}$ dB and minimum aliasing attenuation is approximately $50$ dB. The delay $\tau_T(\omega)$ of the overall filter bank is constant in frequency and is $p\Delta_S = 217$ samples.

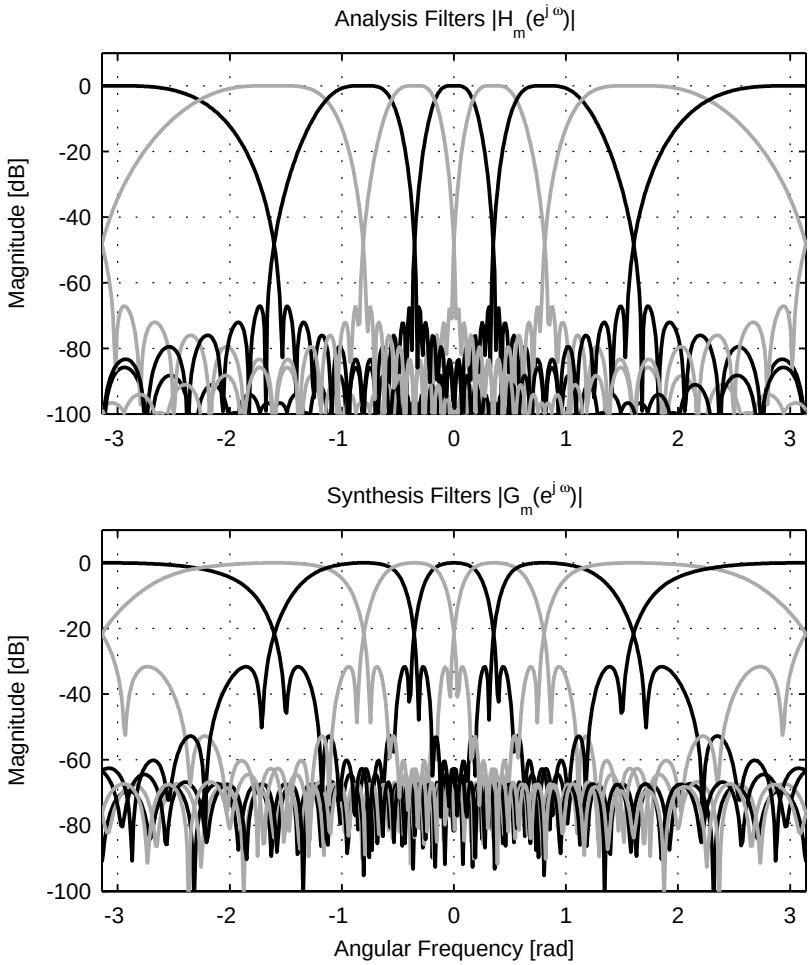


Figure 3.3: **Design Example LS$^2$**. *Magnitude responses of the analysis filters $|H_m(e^{j\omega})|$ and synthesis filters $|G_m(e^{j\omega})|$, for $m = 0, \ldots, M-1$. The analysis and synthesis filter banks are designed with unconstrained quadratic optimization. Phase compensation is used in the synthesis filter bank. The cost function values for the analysis filter bank design are $J_A^I(\mathbf{a}) = -78.4$ dB and $J_A^{II}(\mathbf{a}) = -70.9$ dB.*

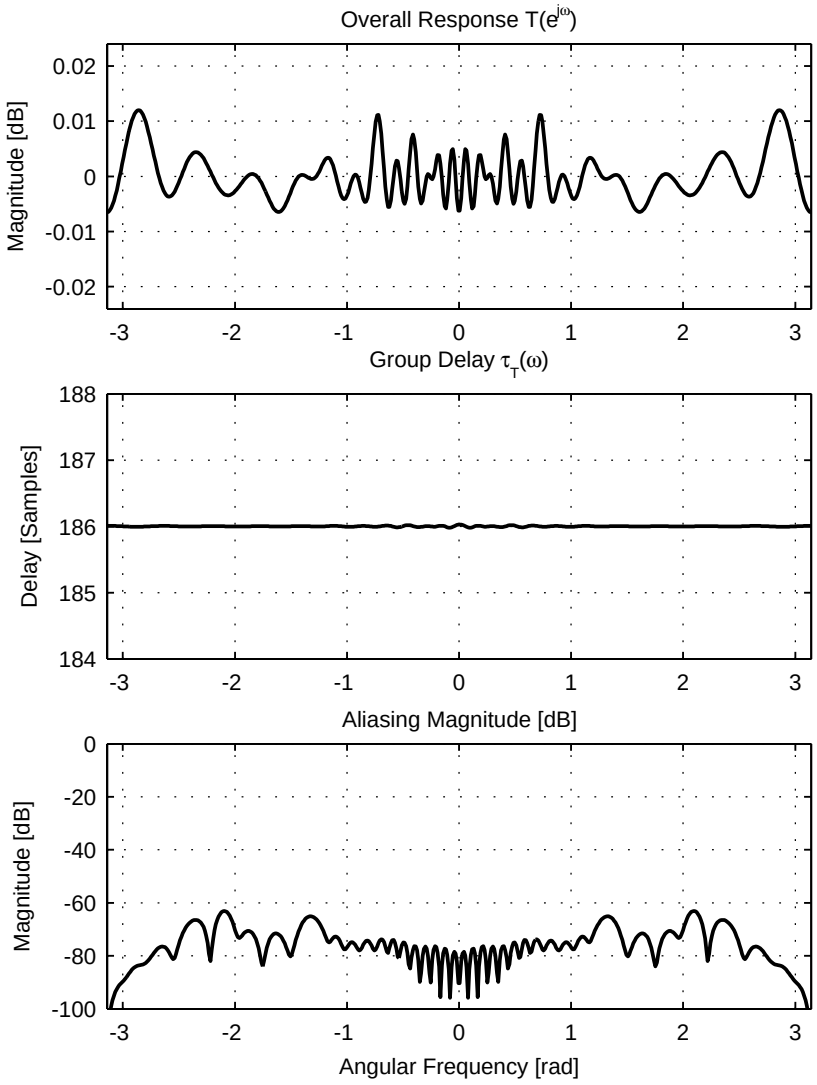


Figure 3.4: **Design Example LS**[2]. *Overall magnitude response* $|T(e^{j\omega})|$*, group delay and maximum aliasing magnitude in the reconstructed output* $S_{avg}(\omega)$*. The cost function values for the synthesis filter bank design are* $J_S^I(\mathbf{b}) = -64.9$ *dB and* $J_S^{II}(\mathbf{b}) = -73.2$ *dB.*

## 3.4 Parameter Analysis

The effect of the passband parameter $\delta$ and the allpass coefficient $\mu$ was studied for the example in Chapter 3.3.1. The passband parameter was varied between $10^{-3}$ and $10^{0}$ and the allpass coefficient was varied between $0.1$ and $0.6$. The minimum of the cost function $J_A(\mathbf{a})$ is plotted as a function of $\delta$ and $\mu$ in Fig. 3.5.

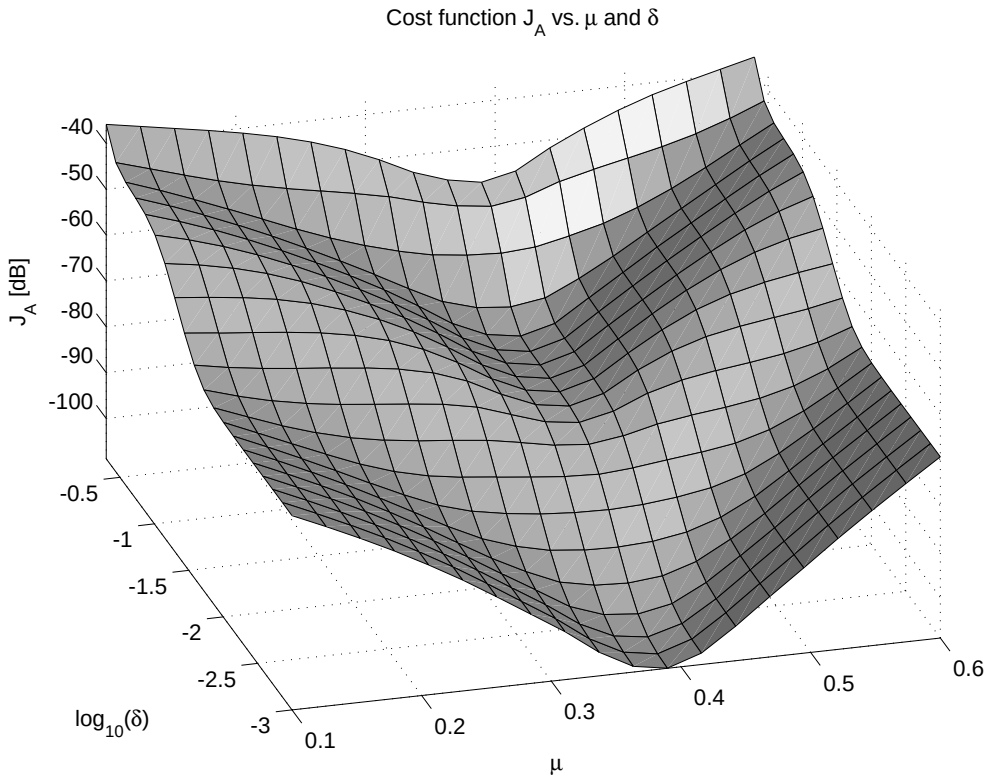


Figure 3.5: *The minimum value of the cost function $J_A(\mathbf{a})$ related to the passband parameter $\delta$ and the allpass coefficient $\mu$. All other parameter settings are the same as in Design LS*[1].

It can be seen that the value of the cost function generally is low when the passband parameter is low, which implies low aliasing levels. For any value of $\delta$, a minimum can be found at a certain value for $\mu$, in this case $\mu \approx 0.4$.

Lower aliasing levels due to high stopband attenuation with low $\delta$ is however at the expense of less control of the passband magnitude and delay. This is illustrated in Fig. 3.6. It can be seen that for low values of $\delta$, the delay is likely to become $\tau_T(\omega) = -\rho'(\omega)\Delta_S$ with $\Delta_S = (NM-1)/2$ although the less delay is specified. This implies a significant trade-off between low aliasing and delay properties, which is controlled by $\delta$.

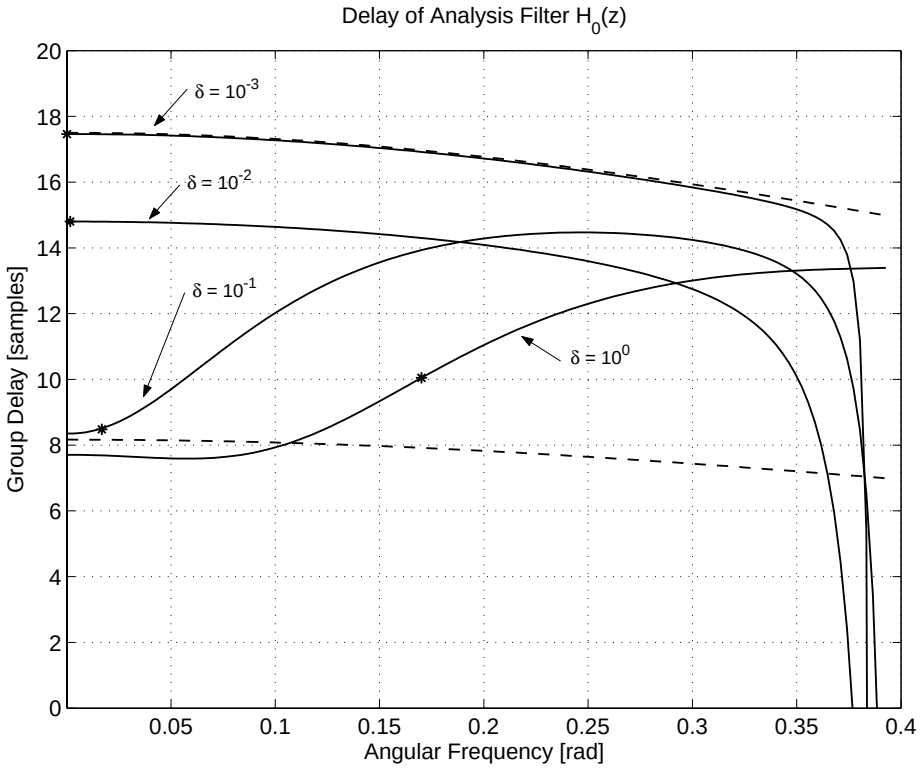


Figure 3.6: *Influence of parameter $\delta$ on the resulting delay of the first analysis filter $H_0(z)$ in the region $\omega = [0, \pi/D_0]$. All parameter settings are the same as for Design Example LS[1], but the desired delay is reduced $\Delta_S = (2M-1)/2$. The dots denotes the passband boundaries for different values of $\delta$. The dashed lower line represents $\tau_H(\omega)$ for $\Delta_A = (2M-1)/2$ and the upper dashed line represents $\tau_H(\omega)$ for $\Delta_A = (4M-1)/2$.*

The influence of the delay parameter $p$ on the design performance, when phase compensation is applied, is illustrated in Fig. 3.7 for $P(z) = z^{-p}$ and $P(z) = z^{-p} + \mu^p$. It can be seen that with the latter choice of $P(z)$, the delay can be reduced by approximately a factor two, while maintaining the performance.

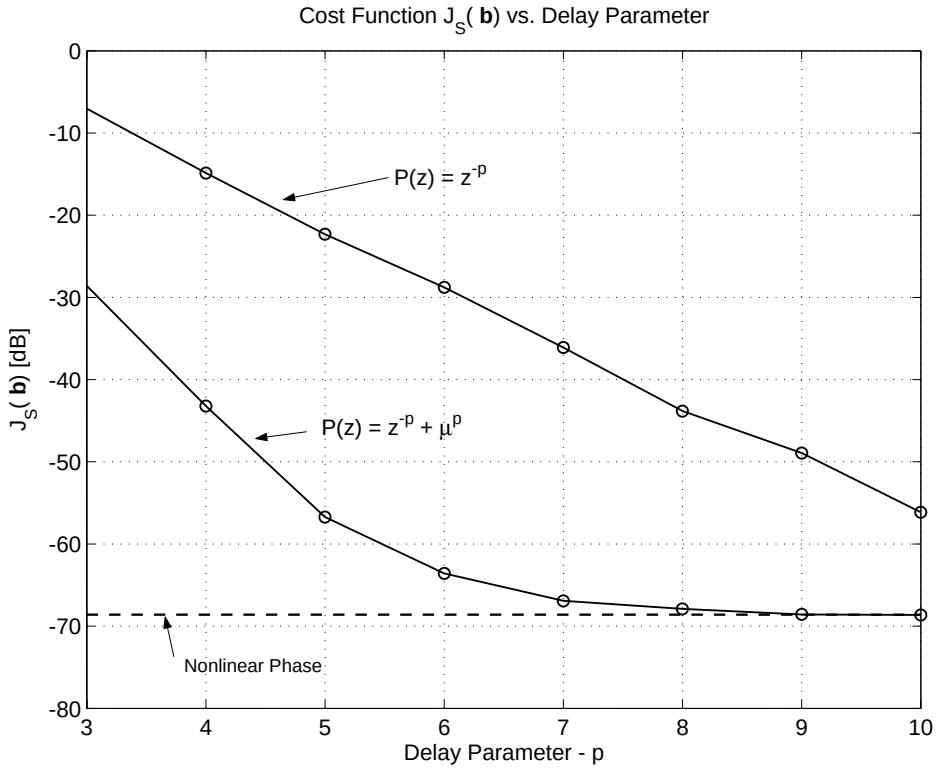


Figure 3.7: *Cost function $J_S(\mathbf{b})$ for different values for the delay parameter $p$. It can be seen that the performance is improved by choosing $P(z) = z^{-p} + \mu^p$ over $P(z) = z^{-p}$ in the synthesis filter bank structure with phase compensation.*

# Chapter 4

# Linear Optimization with Linear Constraints

## 4.1 Analysis Filter Bank Design

A drawback of the unconstrained quadratic optimization method with joint optimization of response and minimization of aliasing energy, is that the resulting amplitude ripple in the analysis filter passbands and the aliasing levels in the subbands cannot be controlled. This can be overcome by imposing design constraints. Furthermore, aliasing can be minimized in a way such that the maximum level is minimized. Both can be achieved by introducing a linear design formulation, with constraints on the maximum passband ripple and minimizing the maximum aliasing level. The design formulation can be written as a finite-dimensional linear program.

The analysis filter bank design criterion with passband ripple constraints is

$$\begin{cases} \min\limits_{\mathbf{a}} \max\limits_{\omega\in\Omega_m^{\mathcal{S}},\forall m} \left|H_m(e^{j\omega})\right| \\ \left|H_m(e^{j\omega}) - H_m^{\mathcal{D}}(e^{j\omega})\right| \leq \sigma, \omega \in \Omega_m^{\mathcal{P}}, \forall m \end{cases} \tag{4.1}$$

where parameter $\sigma$ controls the maximum passband ripple. Using the real rotation theorem [18],

$$|z| \leq \sigma \Leftrightarrow \text{Re}\{ze^{j\theta}\} \leq \sigma, \quad \forall\theta \in [0, 2\pi], \tag{4.2}$$

Eq. (4.1) can be rewritten into the semi-infinite linear program

$$\begin{cases} \min\limits_{\mathbf{a}} J_A^{III} \\ \text{Re}\{H_m(e^{j\omega})e^{j\theta}\} - J_A^{III} \leq 0, \\ \qquad\qquad\qquad\qquad \forall\theta \in [0, 2\pi], \omega \in \Omega_m^{\mathcal{S}}, \forall m \\ \text{Re}\{H_m(e^{j\omega})e^{j\theta}\} \leq \text{Re}\{H_m^{\mathcal{D}}(e^{j\omega})e^{j\theta}\} + \sigma, \\ \qquad\qquad\qquad\qquad \forall\theta \in [0, 2\pi], \omega \in \Omega_m^{\mathcal{P}}, \forall m \end{cases} \tag{4.3}$$

where $J_A^{III}$ is the cost function

$$J_A^{III} = \max_{\omega\in\Omega_m^{\mathcal{S}},\forall m} \left|H_m(e^{j\omega})\right|. \tag{4.4}$$

Using the discrete the frequency domains $\Omega_m^{\mathcal{P}}$, and $\Omega_m^{\mathcal{S}}$, defined in Eq. (3.2), and Eq. (3.4), respectively, and discretization of the rotation angle domain $\theta = 2\pi c/C$, $c = 0, \ldots, C-1$, the formulation in Eq. (4.3) can be approximated by the finite di-

mensional linear program

$$\begin{cases} \min\limits_{\mathbf{a}} J_A^{III} \\ \text{Re}\{e^{j2\pi c/C}\mathbf{\Phi}_m^{\mathcal{S}}\}\mathbf{a} - J_A^{III} & \leq & 0, \forall c, \forall m \\ \text{Re}\{e^{j2\pi c/C}\mathbf{\Phi}_m^{\mathcal{P}}\}\mathbf{a} & \leq & \text{Re}\{e^{j2\pi c/C}\mathbf{H}_m^{\mathcal{D}}\} + \sigma \\ & & \qquad\qquad \forall c, \forall m \end{cases} \tag{4.5}$$

which can be solved using the simplex or similar algorithm. The maximum deviation in the approximation of Eq. (4.1) using $C$ equidistant points, is $1 - \cos(\pi/C)$ [18].

## 4.2 Synthesis Filter Bank Design

A drawback of unconstrained quadratic optimization method for the synthesis filter bank with joint optimization of response and minimization of aliasing is that the resulting amplitude ripple in the overall response and the aliasing levels in the reconstructed output signal cannot be controlled. However, similar to the analysis filter bank design problem, the synthesis filter bank design problem can be formulated as a constrained linear design problem, with constraint on the maximum overall response ripple and minimizing the maximum aliasing level in the reconstructed output signal.

The synthesis filter bank design criterion with overall response ripple constraints is

$$\begin{cases} \min\limits_{\mathbf{b}} \max\limits_{\omega\in\Omega,\forall m,\forall d>0} \left|S_{m,d}(e^{j\omega})\right| \\ \left|T(e^{j\omega}) - T^{\mathcal{D}}(e^{j\omega})\right| \leq \sigma, \omega \in \Omega \end{cases} \tag{4.6}$$

where $\sigma$ is maximum magnitude deviation from unity in the overall response. Introducing the cost function

$$J_S^{III} = \max_{\omega\in\Omega,\forall m,\forall d>0} \left|S_{m,d}(e^{j\omega})\right|, \tag{4.7}$$

and using the real rotation theorem Eq. (4.2), the design formulation in Eq. (4.6) can be rewritten into the semi-infinite linear program

$$\begin{cases} \min\limits_{\mathbf{b}} J_S^{III} \\ \text{Re}\{S_{m,d}(e^{j\omega})e^{j\theta}\} - J_S^{III} & \leq & 0, \\ & & \qquad \forall\theta \in [0, 2\pi], \forall m, \forall d > 0 \\ \text{Re}\{T(e^{j\omega})\} & \leq & \text{Re}\{T^{\mathcal{D}}(e^{j\omega})e^{j\theta}\} + \sigma, \\ & & \qquad \forall\theta \in [0, 2\pi], \omega \in \Omega \end{cases} \tag{4.8}$$

Using the discretized frequency domain $\Omega$, and discretized rotation angle domain

$\theta = 2\pi c/C$, $c = 0, \ldots, C-1$ the formulation can be rewritten into a finite dimensional linear program

$$\begin{cases} \min\limits_{\mathbf{b}} J_S^{III} \\ \mathrm{Re}\{e^{j2\pi c/C}\boldsymbol{\Xi}_{m,d}^{\mathcal{S}}\}\mathbf{b} - J_S^{III} & \leq & 0, \forall c, \forall m, \forall d > 0 \\ \mathrm{Re}\{e^{j2\pi c/C}\boldsymbol{\Psi}\}\mathbf{b} & \leq & \mathrm{Re}\{e^{j2\pi c/C}\mathbf{T}^{\mathcal{D}}\} + \sigma, \forall c \end{cases} \tag{4.9}$$

which can be solved using the simplex algorithm.

## 4.3 Design Examples with Constrained Linear Optimization

The parameter settings for the examples in this section are the same as for the design examples in Chapter 3.3. In both the analysis and synthesis filter bank design, the maximum response ripple is set to $\sigma = 0.01$ and the parameter $C$ is set to $C = 8$.

### 4.3.1 Example without Phase Compensation - LP[1]

Filter banks were designed without phase compensation in the synthesis filter bank. The resulting analysis filters $H_m(z)$ and synthesis filters $G_m(z)$ are shown in Fig. 4.1. The stopbands of the analysis and synthesis filters clearly exhibit the equiripple characteristics. The magnitude and the group delay of the overall response, $T(e^{j\omega})$ and the average magnitude of the aliasing terms $S_{\text{avg}}(\omega)$ are shown in Fig. 4.2. The cost function values are shown in Table 6.

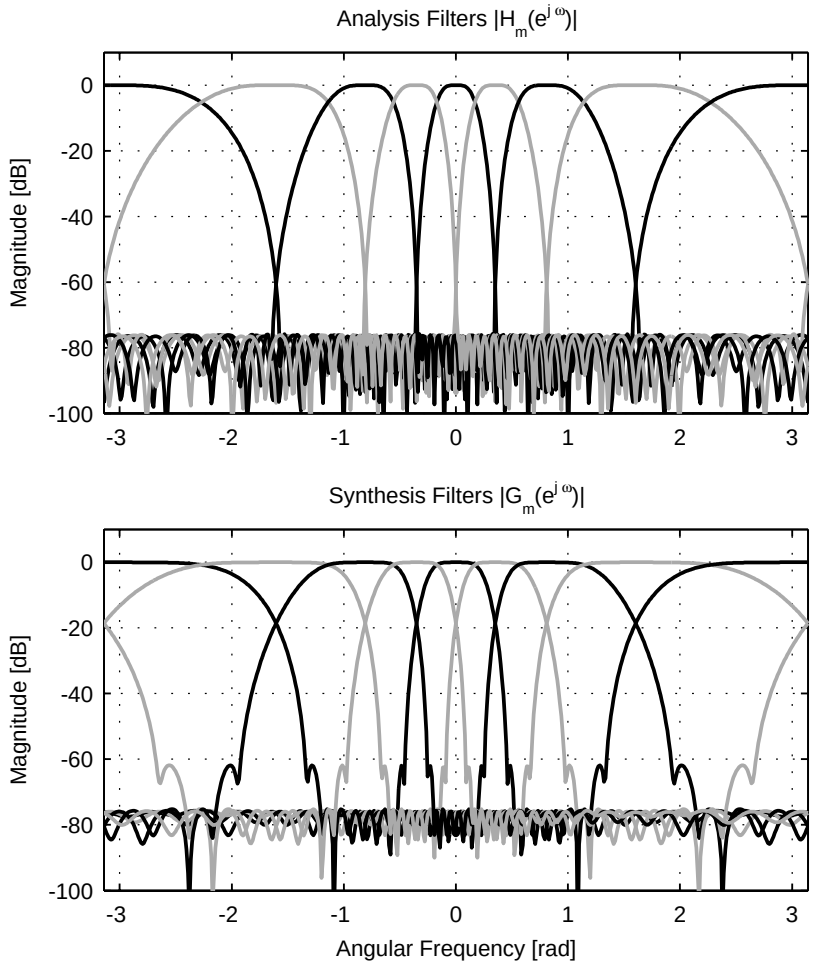


Figure 4.1: **Design Example LP**[1]. *Magnitude responses of the analysis filters* $|H_m(e^{j\omega})|$ *and synthesis filters* $|G_m(e^{j\omega})|$*, for* $m = 0, \ldots, M-1$*. The analysis and synthesis filter banks are designed with linear optimization with linear constraints. There is no phase compensation in the synthesis filter bank. The cost function value for the analysis filter bank design is* $J_A^{III}(\mathbf{a}) = -76.5$ *dB.*

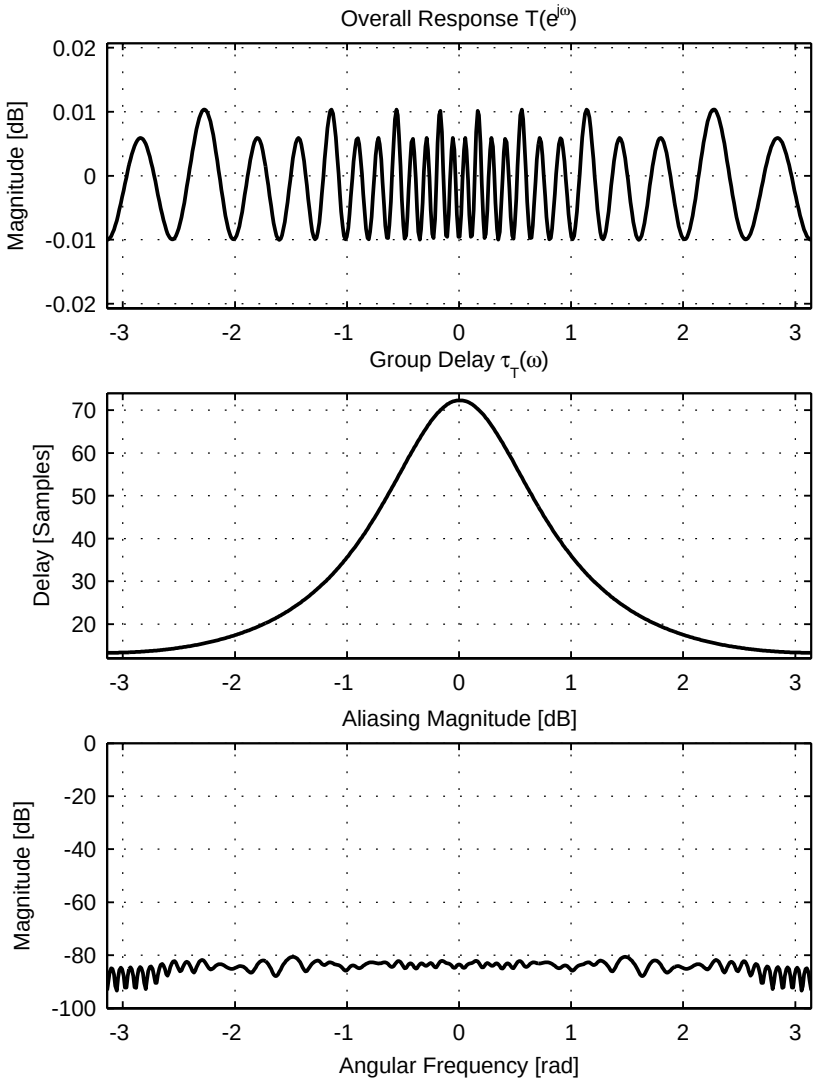


Figure 4.2: **Design Example LP**[1]. *Overall magnitude response* $|T(e^{j\omega})|$*, group delay and maximum output signal aliasing magnitude* $S_{avg}(\omega)$*. The cost function value for the synthesis filter bank design is* $J_S^{III}(\mathbf{b}) = -76.2$ *dB.*

### 4.3.2 Example with Phase Compensation - LP$^2$.

Filter banks were designed using minimax criteria with phase compensation in the synthesis filter bank. The delay parameter for the phase compensation filters is set to $p = 6$. The resulting analysis filters $H_m(z)$ and synthesis filters $G_m(z)$ are shown in Fig. 4.3. The magnitude and the group delay of the overall response, $T(e^{j\omega})$ and the average magnitude of the aliasing terms $S_{\text{avg}}(\omega)$ are shown in Fig. 4.4. The cost function values are shown in Table 6.

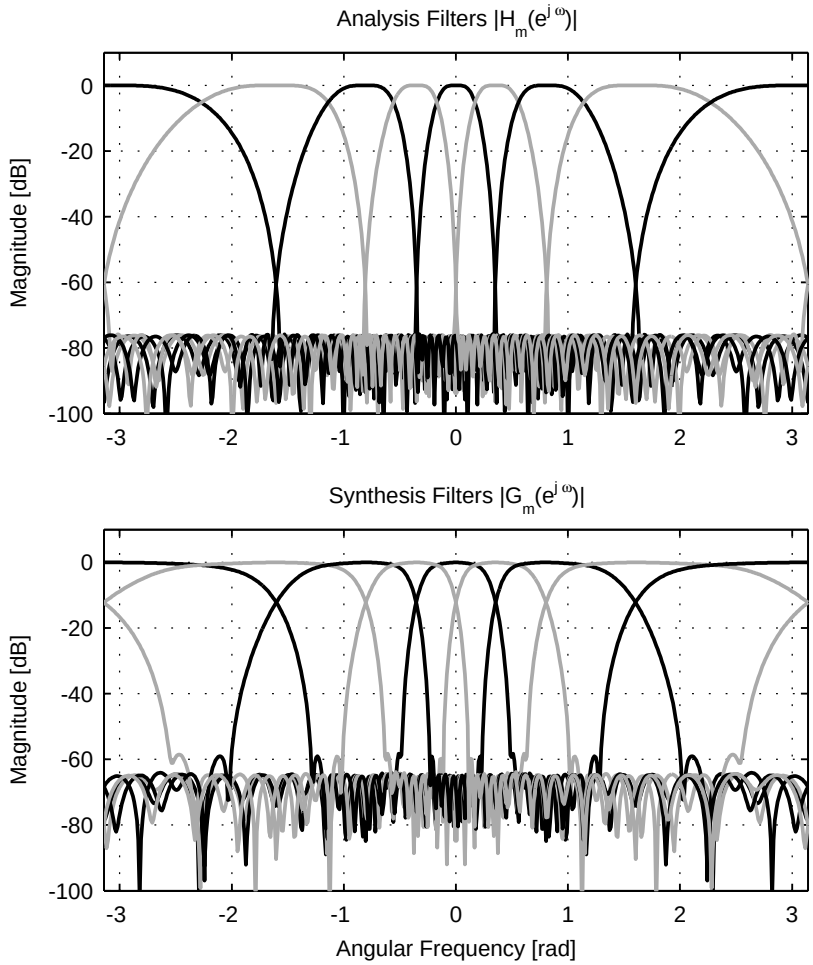


Figure 4.3: **Design Example LP$^2$**. *Magnitude responses of the analysis filters $|H_m(e^{j\omega})|$ and synthesis filters $|G_m(e^{j\omega})|$, for $m = 0, \ldots, M-1$. The analysis and synthesis filter banks are designed with linear optimization with linear constraints. Phase compensation is used in the synthesis filter bank. The cost function value for the analysis filter bank design is $J_A^{III}(\mathbf{a}) = -76.5$ dB.*

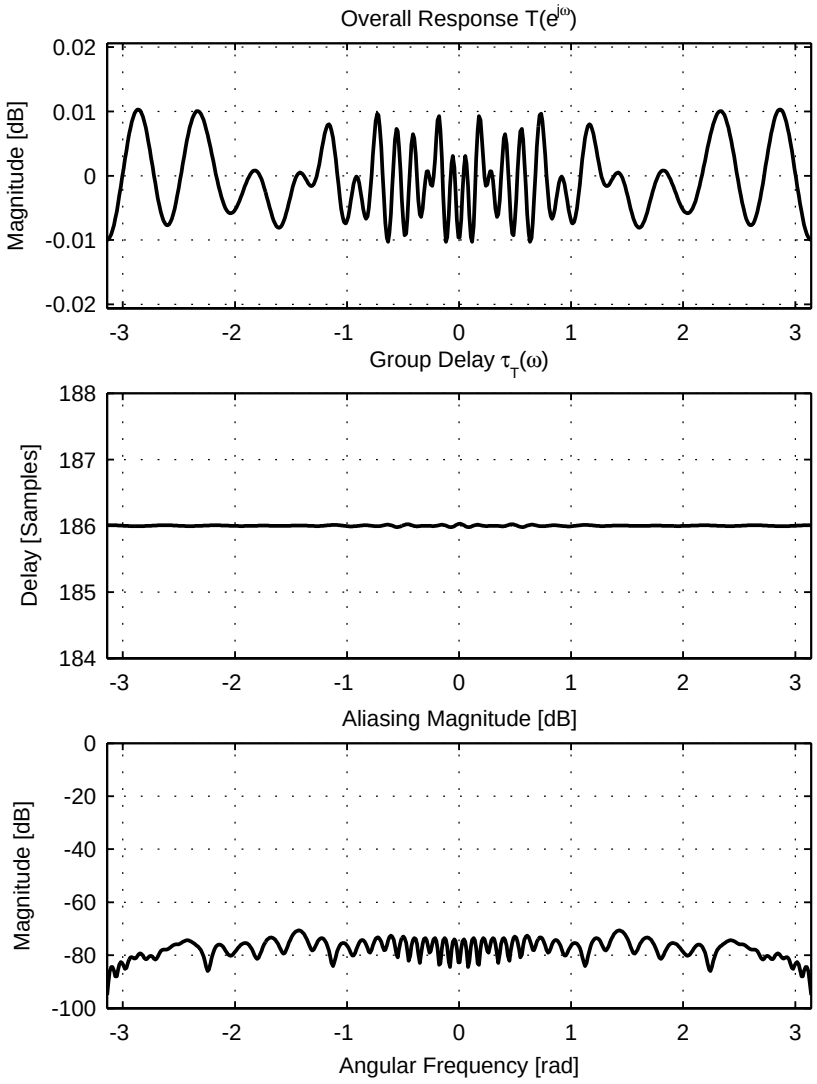


Figure 4.4: **Design Example LP$^2$**. *Overall magnitude response $|T(e^{j\omega})|$, group delay and maximum output signal aliasing magnitude $S_{avg}(\omega)$. The cost function value for the synthesis filter bank design is $J_S^{III}(\mathbf{b}) = -65.1$ dB.*

## 4.4 Parameter Analysis

The trade-off between the maximum response ripple $\sigma$ and the maximum aliasing level $J_S^{III}$ is illustrated for values of $p$ in the range $p \leq 10$ in Fig. 4.5 for $P(z) = z^{-p}$ and Fig. 4.6 for $P(z) = z^{-p} + \mu^p$. Also here, the results show that the delay can be substantially reduced while the aliasing distortion can be maintained at a certain level when the allpass function $P(z) = z^{-p} + \mu^p$ is used in the synthesis filter bank.

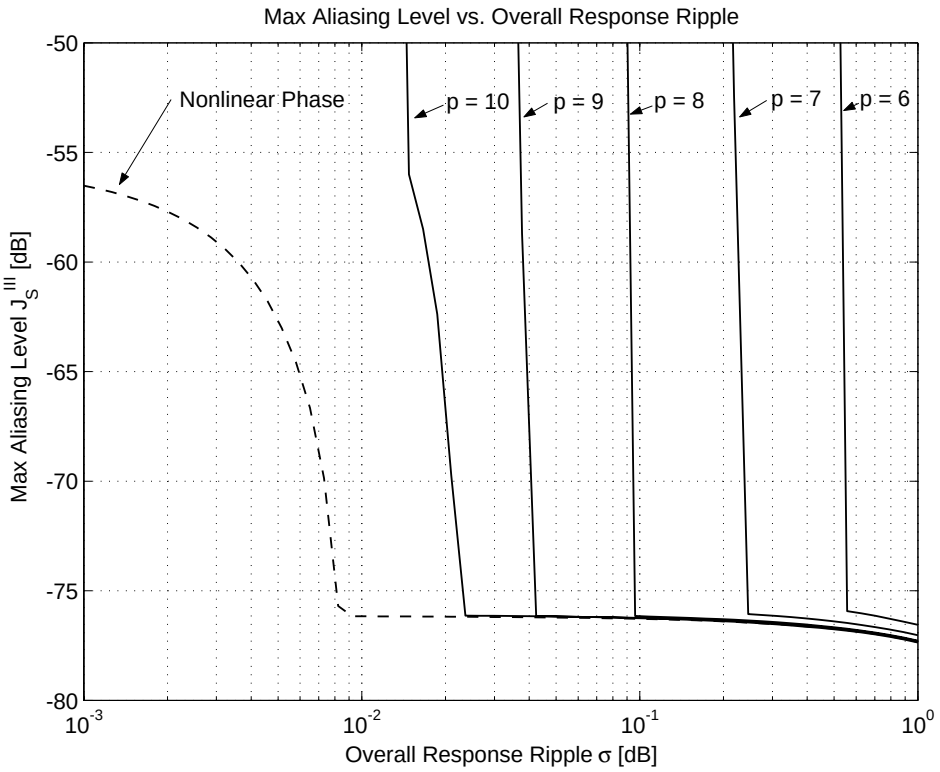


Figure 4.5: *The maximum aliasing level $J_S^{III}$ obtained as a function of the maximum overall response ripple $\sigma$. The function $P(z)$ is a p-sample delay. The dashed line is the non-linear phase case and the other cases are phase compensated with $p \leq 10$.*

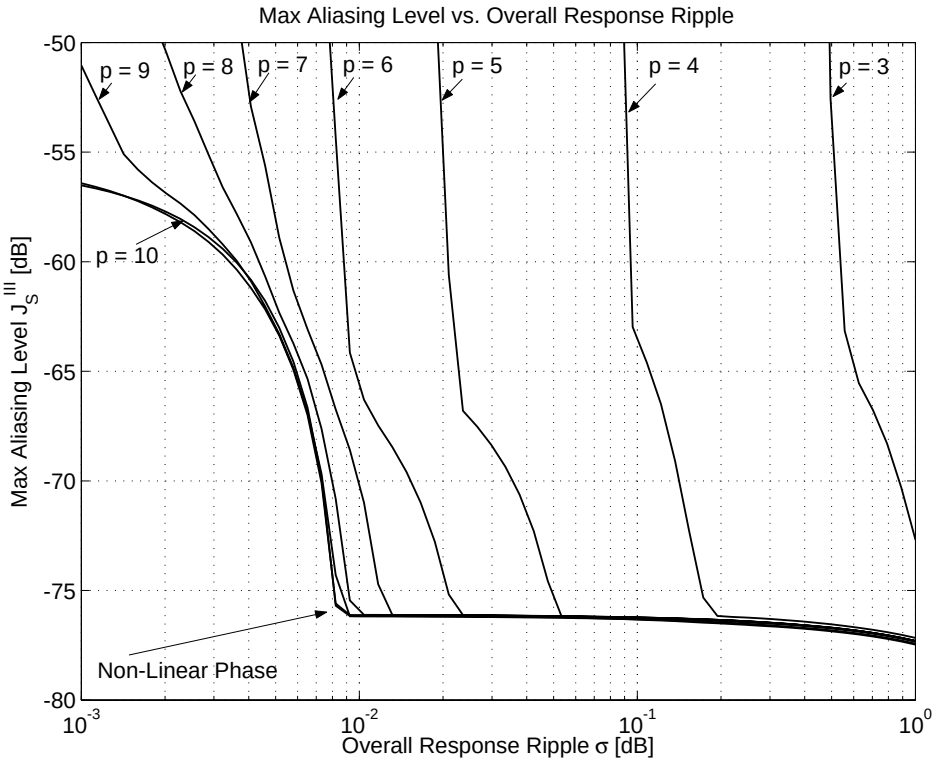


Figure 4.6: *The maximum aliasing level $J_S^{III}$ obtained as a function of the maximum overall response ripple $\sigma$. The function $P(z)$ is chosen as $P(z) = z^{-p} + \mu^p$. The dashed line is the non-linear phase case and the other cases are phase compensated with $p \leq 10$.*

# Chapter 5

# Quadratic Optimization with Linear Constraints

The minimization of aliasing energy on an individual basis with respect to response constraints can be done by combining the quadratic cost functions from Chapter 3 $J_A^{II}(\mathbf{a})$ and $J_S^{II}(\mathbf{b})$ with the linear constraints from Chapter 4, for the analysis and synthesis filter bank respectively.

## 5.1 Analysis Filter Bank Design Criterion

The minimization of subband aliasing energy with respect to constraints on the pass-band ripple can be formulated as

$$\begin{cases} \min\limits_{\mathbf{a}} J_A^{II}(\mathbf{a}) \\ \left|H_m(e^{j\omega}) - H_m^{\mathcal{D}}(e^{j\omega})\right| \leq \sigma, \omega \in \Omega_m^{\mathcal{P}}, \forall m \end{cases} \tag{5.1}$$

Using the matrix notations from Chapters 3 and 4, the formulation in Eq. (5.1) can be approximated by the finite dimensional quadratic program

$$\begin{cases} \min\limits_{\mathbf{a}} \mathbf{a}^T \left\{ \sum\limits_{m=0}^{M-1} {\mathbf{\Phi}_m^{\mathcal{S}}}^H \mathbf{\Phi}_m^{\mathcal{S}} \right\} \mathbf{a} \\ \text{Re}\{e^{j2\pi c/C} \mathbf{\Phi}_m^{\mathcal{P}}\}\mathbf{a} \leq \text{Re}\{e^{j2\pi c/C} \mathbf{H}_m^{\mathcal{D}}\} + \sigma, \ \forall c, \forall m \end{cases} \tag{5.2}$$

## 5.2 Synthesis Filter Bank Design Criterion

The minimization of reconstruction aliasing energy with respect to constraints on the overall response ripple can be formulated as

$$\begin{cases} \min\limits_{\mathbf{b}} J_S^{II}(\mathbf{a}) \\ \left|T(e^{j\omega}) - T^{\mathcal{D}}(e^{j\omega})\right| \leq \sigma, \omega \in \Omega \end{cases} \tag{5.3}$$

Using previous notations, the formulation in Eq. (5.3) can be approximated by the finite dimensional quadratic program

$$\begin{cases} \min\limits_{\mathbf{b}} \mathbf{b}^T \mathbf{\Lambda} \mathbf{b} \\ \text{Re}\{e^{j2\pi c/C} \mathbf{\Psi}\}\mathbf{b} \ \ \leq \ \ \text{Re}\{e^{j2\pi c/C} \mathbf{T}^{\mathcal{D}}\} + \sigma, \forall c \end{cases} \tag{5.4}$$

## 5.3 Design Examples

The parameter settings for the examples in this section are the same as for the design examples in Chapters 3.3 and 4.3. In both the analysis and synthesis filter bank design, the maximum response ripple is set to $\sigma = 0.01$ and parameter $C$ is set to $C = 8$.

### 5.3.1 Example without Phase Compensation - QP[1]

Filter banks are designed without phase compensation in the synthesis filter bank. The resulting analysis filters $H_m(z)$ and synthesis filters $G_m(z)$ are shown in Fig. 5.1. The stopbands of the analysis and synthesis filters clearly exhibit minimum energy characteristics. The magnitude and the group delay of the overall response, $T(e^{j\omega})$ and the average magnitude of the aliasing terms $S_{\text{avg}}(\omega)$ are shown in Fig. 5.2. The cost function values are shown in Table 6.

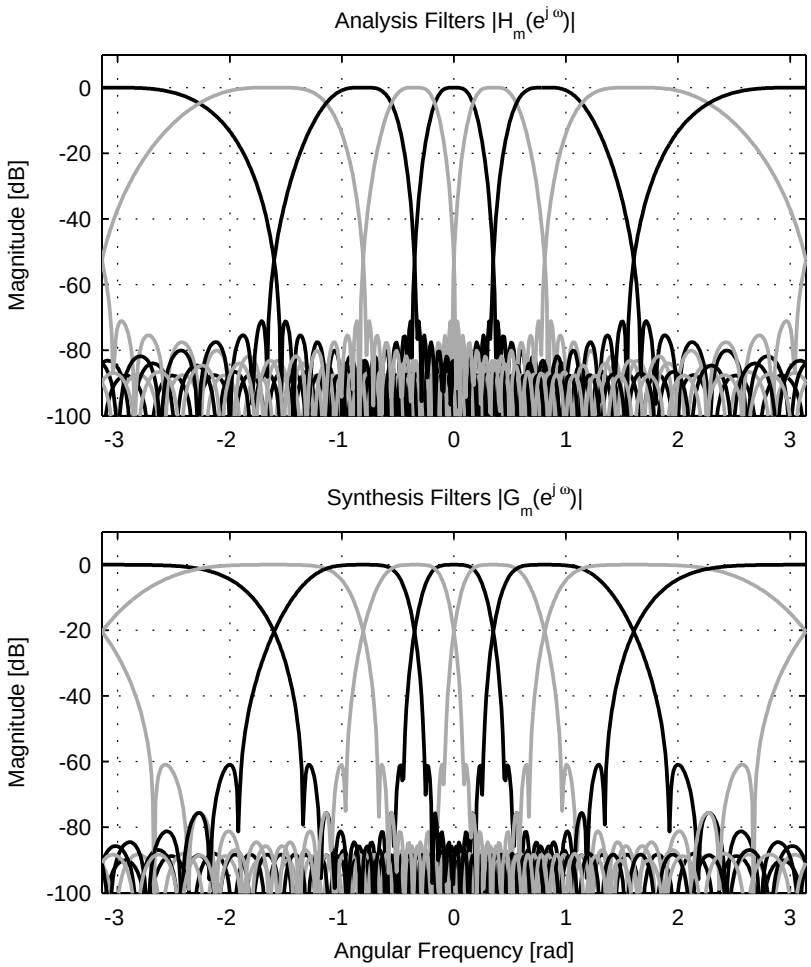


Figure 5.1: **Design Example QP**[1]. *Magnitude responses of the analysis filters* $|H_m(e^{j\omega})|$ *and synthesis filters* $|G_m(e^{j\omega})|$*, for* $m = 0, \ldots, M-1$*. The analysis and synthesis filter banks are designed using quadratic optimization with linear constraints. There is no phase compensation in the synthesis filter bank. The cost function value for the analysis filter bank design is* $J_A^{II}(\mathbf{a}) = -81.6$ *dB.*

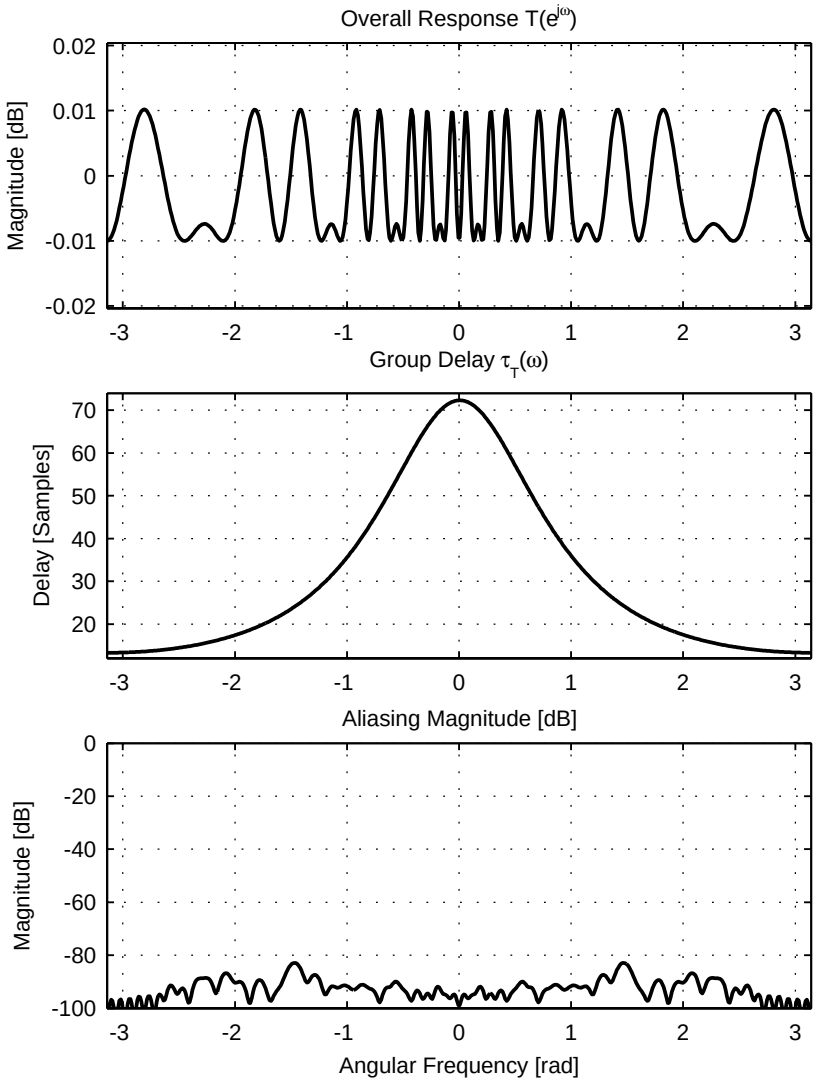


Figure 5.2: **Design Example QP**[1]. *Overall magnitude response* $|T(e^{j\omega})|$*, group delay and maximum output signal aliasing magnitude* $S_{avg}(\omega)$*. The cost function value for the synthesis filter bank design is* $J_S^{II}(\mathbf{b}) = -91.7$ *dB.*

### 5.3.2 Example with Phase Compensation - QP$^2$.

Filter banks are designed without phase compensation in the synthesis filter bank. The delay parameter for the phase compensation filters is set to $p = 6$. The resulting analysis filters $H_m(z)$ and synthesis filters $G_m(z)$ are shown in Fig. 5.3. The magnitude and the group delay of the overall response, $T(e^{j\omega})$ and the average magnitude of the aliasing terms $S_{\text{avg}}(\omega)$ are shown in Fig. 5.4. The cost function values are shown in Table 6.

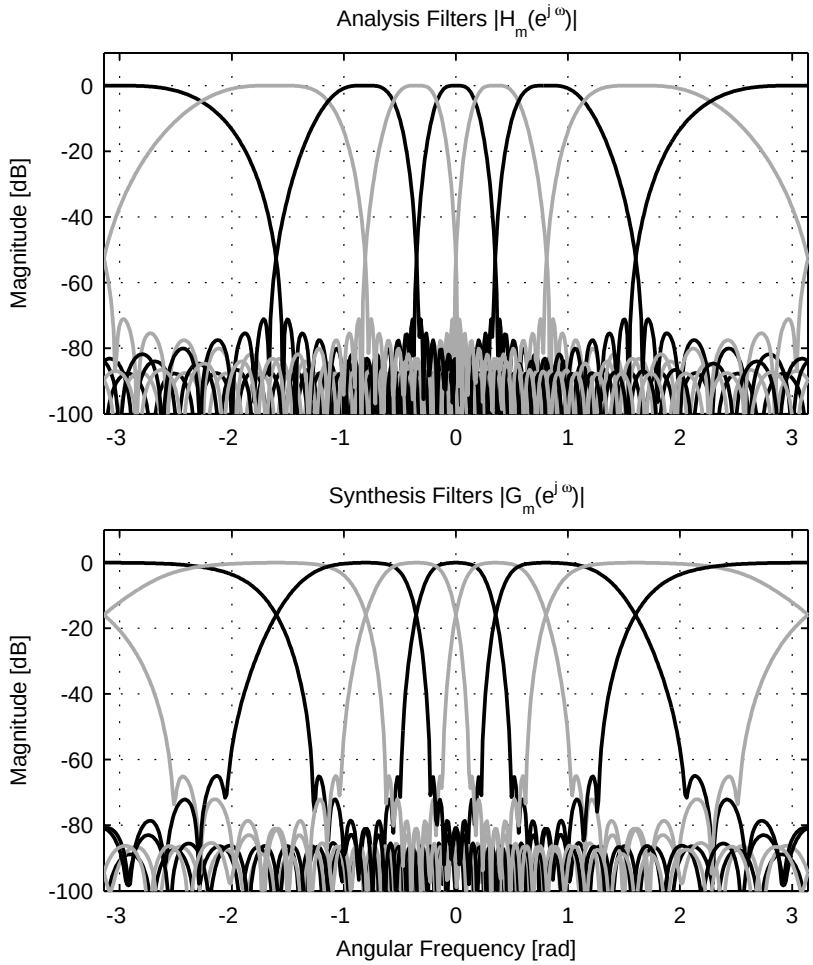


Figure 5.3: **Design Example QP$^2$**. *Magnitude responses of the analysis filters* $|H_m(e^{j\omega})|$ *and synthesis filters* $|G_m(e^{j\omega})|$*, for* $m = 0, \ldots, M-1$*. The analysis and synthesis filter banks are designed using quadratic optimization with linear constraints. Phase compensation is used in the synthesis filter bank. The cost function value for the analysis filter bank design is* $J_A^{II}(\mathbf{a}) = -81.6$ *dB.*

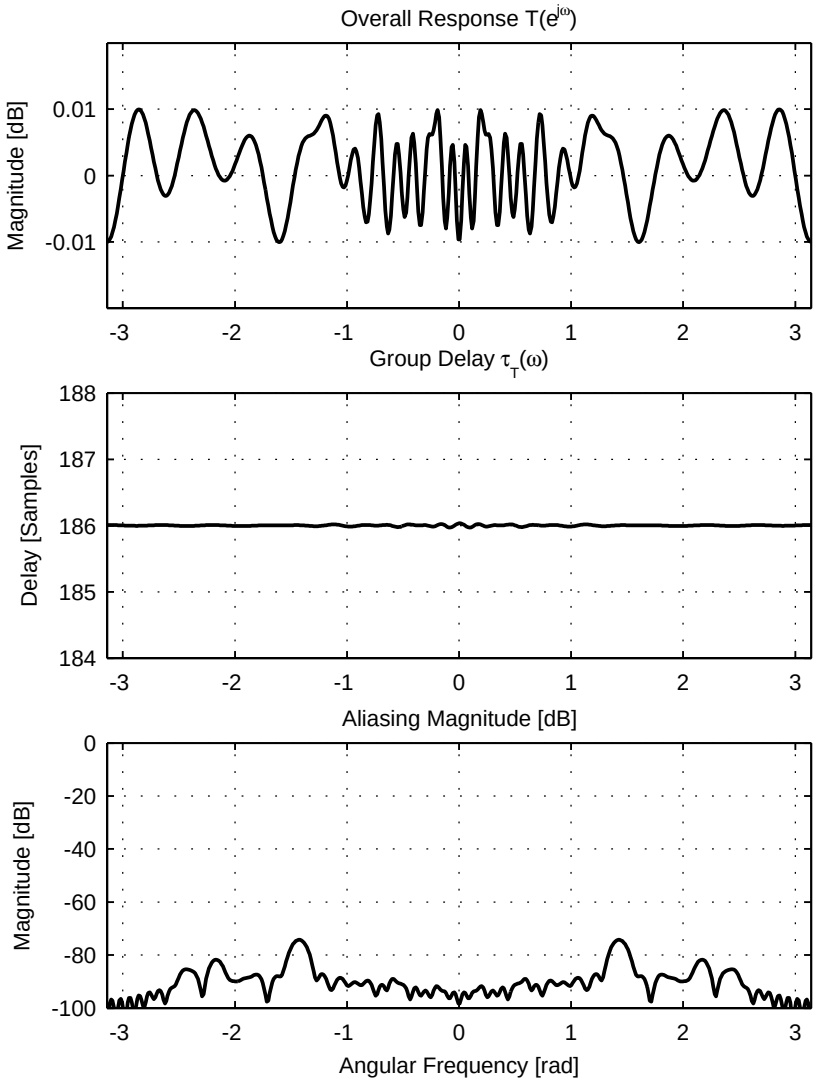


Figure 5.4: **Design Example QP**[2]. *Overall magnitude response* $|T(e^{j\omega})|$*, group delay and maximum output signal aliasing magnitude* $S_{avg}(\omega)$*. The cost function value for the synthesis filter bank design is* $J_S^{II}(\mathbf{b}) = -86.6$ *dB.*

## 5.4 Parameter Analysis

Similar to the parameter analysis of the previous methods, the trade-off between the maximum response ripple $\sigma$ and the aliasing energy $J_S^{II}\mathbf{b}$ is illustrated for values of $p$ in the range $p \leq 10$ in Fig. 5.5 for $P(z) = z^{-p}$ and Fig. 5.6 for $P(z) = z^{-p} + \mu^p$. The results are comparable to the results in Chapter 4.4.

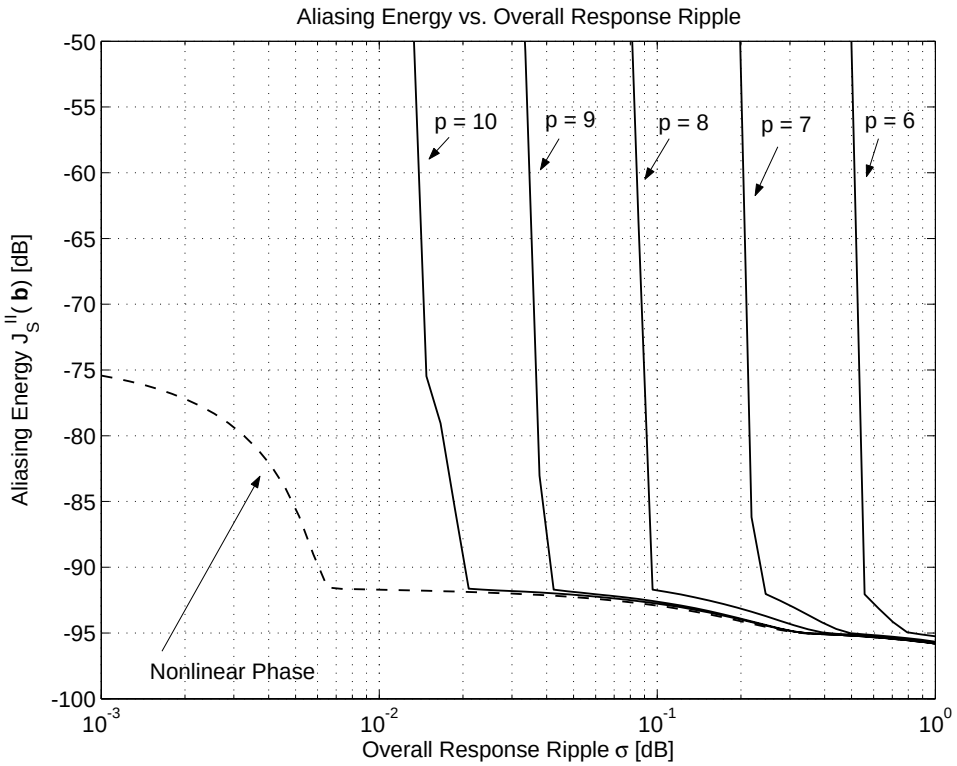


Figure 5.5: *The aliasing energy $J_S^{II}(\mathbf{b})$ obtained as a function of the maximum overall response ripple $\sigma$. The function $P(z)$ is a p-sample delay. The dashed line is the non-linear phase case and the other cases are phase compensated with $p \leq 10$.*

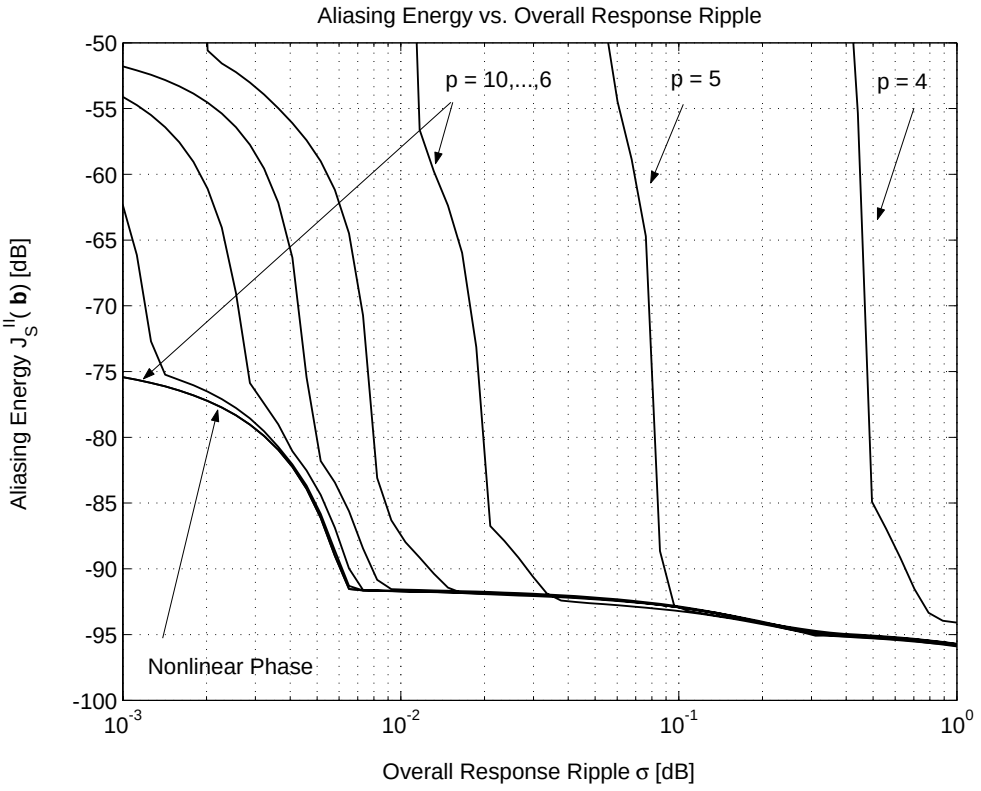


Figure 5.6: *The aliasing energy $J_S^{II}(\mathbf{b})$ obtained as a function of the maximum overall response ripple $\sigma$. The function $P(z)$ chosen as $P(z) = z^{-p} + \mu^p$. The dashed line is the non-linear phase case and the other cases are phase compensated with $p \leq 10$.*

# Chapter 6

# Discussion of Results

In order to compare the performance of the design examples, all cost functions have been evaluated for all design examples and shown in Table 6. The design examples are listed to the left. The filter banks without phase compensation are listed in the upper half of the table and the design examples with phase compensation are listed in the lower half of the table. The analysis filter banks for the two types of design examples are the same, therefore the cost function values are the same. The underlined values denote the cost function which are subject to optimization.

In the $LS^1$ and $LS^2$ design examples it should be noted that the sum of two cost functions is minimized. This means that there is a trade-off between these two cost functions. This can be seen when comparing the quadratic cost functions $J_A^I$, $J_S^I$, $J_A^{II}$, and $J_S^{II}$ for the design examples LP and QP. In the design examples denoted QP, the quadratic cost functions $J_A^{II}$ and $J_S^{II}$ are lower than for the examples denoted LS. Also for the design examples denoted LP, the cost functions $J_A^{II}$ and $J_S^{II}$ are lower than in the examples denoted LS. This may seem unexpected, but it should be noted that for the LP and QP examples, the cost functions $J_A^I$ and $J_S^I$ have a higher value simultaneously. It should be noted that in the design examples QP, the optimization could also be on the quadratic cost functions $J_A^I$ and $J_S^I$, combined with linear constraints on the aliasing levels. The best design in terms of the minimax cost functions $J_A^{III}$ and $J_S^{III}$ are the designs denoted LP, which is an expected result.

The results show that linear and quadratic programming techniques are to be preferred over the unconstrained least squares optimization, since different distortions can be individually minimized and controlled.

| | LS Analysis | | LS Synthesis | | Minimax | |
|---|---|---|---|---|---|---|
| **Design** | $J_A^I(\mathbf{a})$ | $J_A^{II}(\mathbf{a})$ | $J_S^I(\mathbf{b})$ | $J_S^{II}(\mathbf{b})$ | $J_A^{III}(\mathbf{a})$ | $J_S^{III}(\mathbf{b})$ |
| LS[1] | $\underline{-78.4}$ | $\underline{-70.9}$ | $\underline{-84.9}$ | $\underline{-76.2}$ | $-55.9$ | $-55.6$ |
| LP[1] | $-60.0$ | $-76.1$ | $-60.7$ | $-83.7$ | $\underline{-76.5}$ | $\underline{-76.2}$ |
| QP[1] | $-60.2$ | $\underline{-81.6}$ | $-61.2$ | $\underline{-91.7}$ | $-61.7$ | $-74.3$ |
| LS[2] | $\underline{-78.4}$ | $\underline{-70.9}$ | $\underline{-64.9}$ | $\underline{-73.2}$ | $-55.9$ | $-50.0$ |
| LP[2] | $-60.0$ | $-76.1$ | $-62.7$ | $-76.0$ | $\underline{-76.5}$ | $\underline{-65.1}$ |
| QP[2] | $-60.2$ | $\underline{-81.6}$ | $-61.7$ | $\underline{-86.6}$ | $-61.7$ | $-65.5$ |
| | All measures in dB | | | | | |

[1]without phase compensation, [2]with phase compensation.
LS = Least Squares, LP = Linear Optimization, QP = Quadratic Optimization.

Table 6.1: *Cost Function Values for the design examples given in Chapters 3.3, 4.3 and 5.3. For the sake of comparison, all cost functions are evaluated for all designs. The underlined values denote the cost functions that are subject to optimization.*

# Chapter 7

# Computational Complexity

In this chapter the filter bank complexity for real-valued signals, and the complexity of the design methods is briefly discussed.

## 7.1 Filter Bank Complexity

The allpass functions can be implemented by using the one-multiplier structure depicted in Fig. 7.1. This structure has one real multiplication and 3 real additions. The

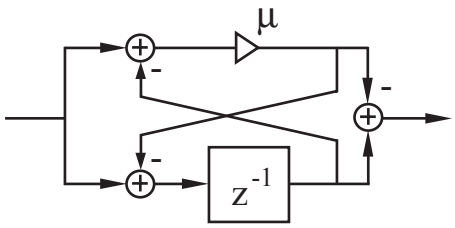


Figure 7.1: *One-multiplier implementation of allpass function* $Q(z)$.

total number of allpass functions is $MN-1$ which implies $MN-1$ multiplications and $3(MN-1)$ additions. The polyphase coefficients require $MN$ multiplications and $M(N-1)$ additions. When assuming a real-valued input signal, the FFT and IFFT require $M \log_2 M$ multiplications and $M \log_2 M$ additions each. The decimation gain compensation are $M-2$ complex multipliers and 2 real multipliers (for real-valued subbands $m = 0$ and $m = M/2$), in decimated subbands. Normalized with the decimation rate, this implies

$$\frac{1}{D_0} + \frac{1}{D_{M/2}} + 4 \sum_{d=1}^{M/2-1} \frac{1}{D_m} \tag{7.1}$$

real multiplications. The synthesis polyphase coefficients require $ML$ multiplications. In the nonlinear phase case, the allpass-and-sum chain is implemented with $ML-1$ multiplications and $4(ML-1)$ additions. In the case with phase compensation and $P(z) = z^{-p} + \mu^p$, each allpass function requires one multiplication and one addition. Each phase compensation filter $R^k(z)$, for $k = 1, \ldots, ML-1$ requires $kp+1$ multiplications and $kp+2$ additions, this gives a total of

$$\sum_{k=1}^{ML-1} (kp+1) = \frac{1}{2}p(ML)^2 + (1 - \frac{1}{2}p)(ML) - 1 \tag{7.2}$$

real multiplications and the same number plus $ML - 1$ real additions.

| | **Real Multiplications** |
|---|---|
| Allpass Chain | $MN - 1$ |
| Polyphase Coefficients | $MN$ |
| IFFT | $M \log_2 M$ |
| Compensation for Decimation | $\frac{1}{D_0} + \frac{1}{D_{M/2}} + 4 \sum_{d=1}^{M/2-1} \frac{1}{D_m}$ |
| FFT | $M \log_2 M$ |
| Polyphase Coefficients | $ML$ |
| Phase Compensation[1] | $\frac{1}{2}p(ML)^2 + (1 - \frac{1}{2}p)(ML) - 1$ |
| Allpass Chain[1] | $ML - 1$ |
| Allpass Chain[2] | $ML - 1$ |

[1]with phase compensation, [2]without phase compensation

Table 7.1: *Computational complexity for real-valued signals. The table shows the number of real multiplications*

| | **Real Additions** |
|---|---|
| Allpass Chain | $3(MN - 1)$ |
| Polyphase Coefficients | $M(N - 1)$ |
| IFFT | $M \log_2 M$ |
| Compensation for Decimation | — |
| FFT | $M \log_2 M$ |
| Polyphase Coefficients | — |
| Phase Compensation[1] | $\frac{1}{2}p(ML)^2 + (2 - \frac{1}{2}p)(ML) - 2$ |
| Allpass Chain[1] | $2(ML - 1)$ |
| Allpass Chain[2] | $4(ML - 1)$ |

[1]with phase compensation, [2]without phase compensation

Table 7.2: *Computational complexity for real-valued signals. The table shows the number of real additions*

The number of multiplications and additions is summarized in Tables 7.1 and 7.1. The complexity relative to the uniform DFT filter bank is illustrated in Fig. 7.2. It can be seen that the complexity for uncompensated filter banks with nonlinear phase is less than twice as high and is going towards the complexity for uniform filter banks for an increasing number of subbands. The relative complexity for phase-compensated filter banks however is large, linearly increasing with the number of subbands and the delay parameter $p$, due to the phase compensation filters.

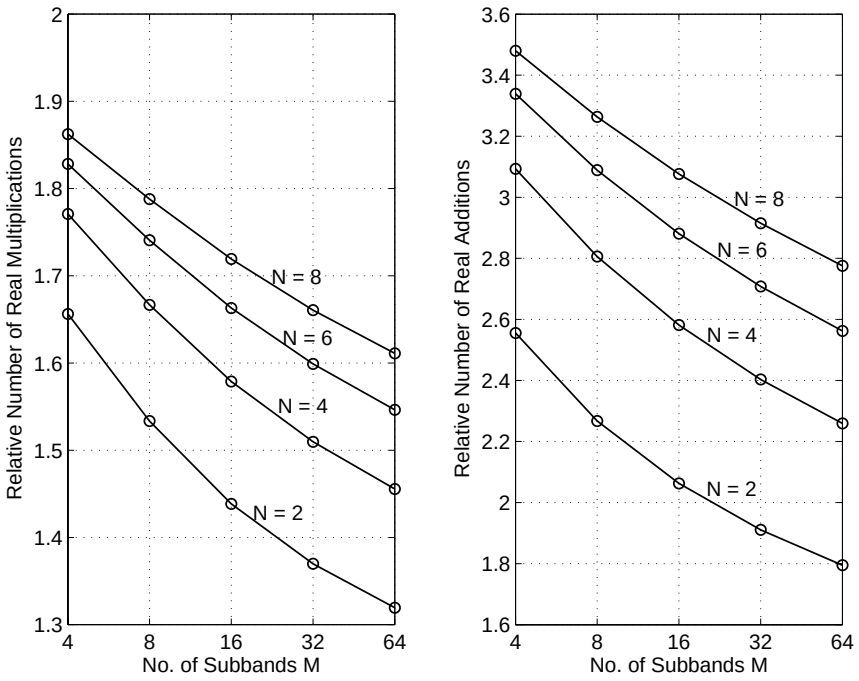


Figure 7.2: *Real multiplications and real additions for nonuniform filter banks with uncompensated phase as functions of the number of subbands normalized with the numbers for a uniform DFT filter bank. Different filter lengths are shown,* $N = L = 2, 4, 6, 8$.

## 7.2 Design Method Complexity

For the sake of comparison of the complexity of the different design methods, the computation times were measured for the design examples presented in the previous chapters. The computations are performed using *Matlab*. The measured computation times for the initialization and the optimization methods, relative to the unconstrained quadratic optimization method, are given in Table 7.2. Clearly, the linear optimization method requires much computation time, while computation time of the constrained quadratic optimization is more comparable to the unconstrained quadratic optimization method. The complexity of the constrained methods is highly dependent on the number of constraints. For the quadratic optimization method, the complexity tends to increase linearly with the number of constraints. For the linear optimization method, the complexity increases at a faster rate.

| | **LS** | **LP** | **QP** |
|---|---|---|---|
| Analysis – Init | $1.00 \cdot 10^0$ | $5.29 \cdot 10^0$ | $1.07 \cdot 10^0$ |
| Analysis – Opt | $1.00 \cdot 10^0$ | $2.25 \cdot 10^3$ | $6.00 \cdot 10^1$ |
| Synthesis – Init | $1.00 \cdot 10^0$ | $1.15 \cdot 10^0$ | $0.92 \cdot 10^0$ |
| Synthesis – Opt | $1.00 \cdot 10^0$ | $2.97 \cdot 10^3$ | $8.06 \cdot 10^1$ |
| | All measures in seconds | | |

LS = Least Squares Unconstrained Quadratic Optimization,
LP = Constrained Linear Optimization,
QP = Constrained Quadratic Optimization.

Table 7.3: *Relative computation time of the design methods initialization and optimization stages.*

# Chapter 8

# Conclusion

In this paper, two stage design methods are presented for the design of nonuniform filter banks using frequency domain criteria for applications such as subband adaptive filtering and subband coding. The polyphase structure with allpass functions is used with or without the compensation of nonlinear phase in the synthesis filter bank. One of the design objectives of the proposed method is to minimize the magnitude of all aliasing components individually, such that aliasing distortion is minimized although phase alterations occur in the subbands as in subband adaptive filtering. Design examples are given of filter banks with increasing bandwidth with a comparison of the results obtained with different design criteria.

# Chapter 9

# Appendix

## 9.1 Derivation of Phase Function $\rho(\omega)$ in Eq. (2.3)

The Fourier transform $Q(e^{j\omega})$, with real-valued coefficient $\mu$, is

$$\begin{aligned} Q(e^{j\omega}) &= \frac{-\mu + e^{-j\omega}}{1 - \mu e^{-j\omega}} && (9.1)\\ &= \frac{-\mu e^{j\frac{\omega}{2}} + e^{-j\frac{\omega}{2}}}{e^{j\frac{\omega}{2}} - \mu e^{-j\frac{\omega}{2}}} && (9.2)\\ &= \frac{(1-\mu)\cos\frac{\omega}{2} - j(1+\mu)\sin\frac{\omega}{2}}{(1-\mu)\cos\frac{\omega}{2} + j(1+\mu)\sin\frac{\omega}{2}} && (9.3) \end{aligned}$$

With $Q(e^{j\omega}) = e^{j\rho(\omega)}$, the phase function $\rho(\omega)$ is

$$\begin{aligned} \rho(\omega) &= \arctan\frac{-(1+\mu)\sin\frac{\omega}{2}}{(1-\mu)\cos\frac{\omega}{2}} + \ldots \\ &\qquad \ldots - \arctan\frac{(1+\mu)\sin\frac{\omega}{2}}{(1-\mu)\cos\frac{\omega}{2}} && (9.4)\\ &= -2\arctan\left(\frac{1+\mu}{1-\mu}\tan\frac{\omega}{2}\right) && (9.5) \end{aligned}$$

## 9.2 Derivation of the Group Delay $\tau_Q(\omega)$ in Eq. (2.4)

The group delay of $Q(e^{j\omega})$ is found by taking the first derivative of the phase function $\rho(\omega)$

$$\begin{aligned} \tau(\omega) &= -\frac{d\rho(\omega)}{d\omega} && (9.6)\\ &= 2\frac{d}{d\omega}\arctan\left(\frac{1+\mu}{1-\mu}\tan\frac{\omega}{2}\right) && (9.7)\\ &= \frac{2\cdot\frac{1+\mu}{1-\mu}\cdot\frac{d}{d\omega}\tan\frac{\omega}{2}}{1+\left(\frac{1+\mu}{1-\mu}\right)^2\tan^2\frac{\omega}{2}} && (9.8)\\ &= \frac{\frac{1+\mu}{1-\mu}\left(1+\tan^2\frac{\omega}{2}\right)}{1+\left(\frac{1+\mu}{1-\mu}\right)^2\tan^2\frac{\omega}{2}} && (9.9) \end{aligned}$$

# Bibliography


[1] J. Rothweiler, "Polyphase Quadrature Filters – A New Subband Coding Technique," in *IEEE International Conference on Acoustics, Speech, and Signal Processing*, October 1983, pp. 1280–1283.

[2] M. Vetterli, "Filter Banks Allowing for Perfect Reconstruction," *Elsevier Signal Processing*, vol. 10, pp. 219–244, April 1986.

[3] P. P. Vaidyanathan, *Multirate Systems and Filter Banks*, Prentice-Hall, 1993.

[4] J. M. de Haan, N. Grbić, I. Claesson, and S. Nordholm, "Filter Bank Design for Subband Adaptive Microphone Arrays," *IEEE Transactions on Speech and Audio Processing*, vol. 11, pp. 14–23, January 2003.

[5] H. Gustafsson, S. Nordholm, and I. Claesson, "Spectral Subtraction using Reduced Delay Convolution and Adaptive Averaging," *IEEE Transactions on Speech and Audio Processing*, vol. 9, pp. 799–807, November 2001.

[6] J. M. de Haan, N. Grbić, I. Claesson, and S. Nordholm, "Design of Oversampled Uniform DFT Filter Banks with Delay Specification using Quadratic Optimization," in *IEEE International Conference on Acoustics, Speech, and Signal Processing*, May 2001, pp. 3633–3636.

[7] J. O. Smith III and J. S. Abel, "Bark and ERB Bilinear Transforms," *IEEE Transactions on Speech and Audio Processing*, vol. 7, pp. 697–708, November 1999.

[8] T. Gülzow, A. Engelsberg, and U. Heute, "Comparison of a Discrete Wavelet Transformation and a Nonuniform Polyphase Filter Bank Applied to Spectral Subtraction Speech Enhancement," *Elsevier Signal Processing*, pp. 5–19, 1998.

[9] J. M. de Haan, N. Grbić, I. Claesson, and S. Nordholm, "Design and Evaluation of Nonuniform DFT Filter Banks in Subband Microphone Arrays," in *IEEE International Conference on Acoustics, Speech, and Signal Processing*, May 2002, pp. 1173 –1176.

[10] A. G. Constantinides, "Spectral Transformations for Digital Filters," *IEE Proceedings*, vol. 117, pp. 1585–1590, 1970.

[11] M. Kappelan, B. Strauss, and P. Vary, "Flexible Nonuniform Filter Banks using Allpass Transformation of Multiple Order," in *EURASIP European Signal Processing Conference*, 1996, pp. 1745–1748.

[12] G. Evangelista and S. Cavaliere, "Frequency-Warped Filter Banks and Wavelet Transforms: A Discrete-Time Approach via Laguerre Expansion," *IEEE Transactions on Signal Processing*, vol. 46, pp. 2638–2650, October 1998.

[13] E. Galijašević and J. Kliewer, "Non-Uniform Near-Perfect Reconstruction Oversampled DFT Filter Banks Based on Allpass Transforms," in *IEEE Proceedings of the ninth DSP Workshop*, October 2000.

[14] D. B. H. Tay, "Least Squares Design of the Class of Triplet Halfband Filter Banks," in *IEEE International Symposium on Circuits and Systems*, 2001, vol. 2, pp. 481–484.

[15] M. Rossi, J.-Y. Zhang, and W. Steenaart, "Iterative Least Squares Design of Perfect Reconstruction QMF Banks," in *Proceedings of the Canadian Conference on Electrical and Computer Engineering*, 1996, vol. 2, pp. 762–765.

[16] D. B. H. Tay, "Two Stage, Least Squares Design of Biorthogonal Filter Banks," in *IEEE International Symposium on Circuits and Systems*, 2000, vol. 1, pp. 591–594.

[17] E. Galijašević and J. Kliewer, "Design of Allpass-Based Non-Uniform Oversampled DFT Filter Banks," in *IEEE International Conference on Acoustics, Speech and Signal Processing*, May 2002, pp. 1181–1184.

[18] T. W. Parks and C. S. Burrus, *Digital Filter Design*, John Wiley and Sons, 1987.


Design of Nonuniform Filter Banks with Frequency Domain Criteria
Jan Mark de Haan, Sven Nordholm, Ingvar Claesson

ISSN 1103-1581
ISRN BTH-RES--03/04--SE

Copyright © 2004 by individual authors
All rights reserved
Printed by Kaserntryckeriet AB, Karlskrona 2004